

Analytical Models for Sliding Interfaces Associated with Fibre Fractures or Matrix Cracks

L. N. McCartney¹

Abstract: Analytical stress transfer models are described that enable estimates to be made of the stress and displacement fields that are associated with fibre fractures or matrix cracks in unidirectional fibre reinforced composites. The models represent a clear improvement on popular shear-lag based methodologies. The model takes account of thermal residual stresses, and is based on simplifying assumptions that the axial stress in the fibre is independent of the radial coordinate, and similarly for the matrix. A representation for both the stress and displacement fields is derived that satisfies exactly the equilibrium equations, the required interface continuity equations for displacement and tractions, and all stress-strain equations except for the one that relates to axial deformation. In addition, the representation is such that the Reissner energy functional has a stationary value provided that averaged axial stress-strain relations for the fibre and matrix are satisfied. The improved representation is fully consistent with variational mechanics and provides both the stress and displacement distributions in the fibre and the matrix. For isolated or interacting fibre fractures or matrix cracks, interface sliding is considered where two types of condition are investigated. Firstly, it is assumed that the shear stress is uniform within the sliding region, and a small transition zone is included in the model in order that essential zero traction conditions can be satisfied on the crack surfaces. Secondly, it is assumed that stress transfer in the sliding region is controlled by Coulomb friction. Illustrative predictions are made for an example polymer composite, although the methodology presented is equally applicable to other types of composite (e.g. metal and ceramic matrix composites).

Keywords: Interface, sliding, stress, displacement, friction, stress transfer.

1 Introduction

For unidirectional polymer composites, the fibre fracture is perhaps the most important damage mode, as it can be the precursor to progressive damage growth that

¹ Materials Division, National Physical Laboratory, Teddington, Middx. UK, TW11 0LW.

leads on to the catastrophic failure of the composite. Fibre fracture for weakly bonded composites is often accompanied by the formation of fibre/matrix sliding zones that affect the stress transfer between fibre and matrix, and the performance of the composite in directions normal to the fibre direction. For high temperature brittle matrix composites, the most important damage mode is matrix cracking in a direction normal to the fibre direction. The matrix cracks can be bridged by a number of intact fibres and the opening of the cracks is affected by the degree of fibre/matrix sliding.

To understand these damage modes it is essential that a reliable analysis is undertaken so that stress-transfer between fibres and matrix is adequately modelled. A concentric cylinder model is often used to analyse fibre fractures and matrix cracking, where stress transfer is estimated between two concentric cylinders and where the inner cylinder represents the fibre and the outer cylinder represents the matrix. Historically, shear-lag theories were first used for this purpose, as discussed in detail by Nairn (1997) for the special case where the matrix remains perfectly bonded to the fibres. He critically assessed shear-lag methods which have frequently been used in the literature to analyse fibre/matrix stress transfer. He concluded that shear-lag methods provide poor estimates of shear stresses and energy release rates, and cannot be used for low fibre volume fractions. An additional point, rarely noticed, is that shear-lag methods do not take account of interaction effects that arise when fractures are sufficiently close together. For brittle-matrix composites where interface sliding is a very important mechanism, a shear-lag model was the basis of ACK theory [Aveston, Cooper and Kelly (1971)], when using an energy balance method to predict the conditions for matrix cracking when it is accompanied by fibre/matrix sliding characterised by a uniform interfacial shear stress (see also [McCartney (1987, 1992b,a)]).

Hutchinson and Jensen (1990) avoided the use of a shear-lag model by using the well-known Lamé solution, together with mode II fracture mechanics principles, to consider matrix cracking for cases where frictional slip occurs at the fibre/matrix interfaces characterised by either a uniform interfacial shear stress or by the Coulomb friction law. Their approach estimates a 'steady state' energy release rate using a method that does not consider the variation of the stress field in the direction of the fibres, but only the stress states far 'upstream' and far 'downstream' relative to the fracture location. To obtain more accurate solutions than shear-lag methods, Nairn (1992) used a variational calculation based on the principle of minimising the complementary energy to develop a solution for the stress field only for the special case where the fibre/matrix interface remains perfectly bonded. He applied the model to the analysis of single-fibre fibre-pull-out tests and micro-drop debond tests.

In this paper, an axisymmetric model is considered subject to applied axial load

distributions that gives rise to axial stress transfer between the concentric cylinders through the action of distributed shear stresses on the interface between the two cylinders. The model is constructed so that the cylinders can be made of different transversely isotropic materials. The model takes full account of the effects of the thermal residual stresses induced in the system during manufacture as a result of the difference in thermal expansion behaviour of the fibre and matrix. The solution technique, which is an improvement of an earlier stress transfer model [McCartney (1989)], is briefly described in reference [McCartney (1999)]. The solution of the stress transfer problem involves the development of an ordinary differential equation that can be solved by analytical methods, and enables subsequent calculation of the stress and displacement distributions throughout the system. The axisymmetric model of stress transfer leads to stationary values of the Reissner energy functional [Reissner (1950)] so that the stress and displacement distribution derived from the model would also result from carrying out a corresponding variational calculation. Thus, the stress transfer model is the best that can be developed based upon the single fundamental assumption that axial stresses in each cylinder are independent of the radial coordinate. This assumption is not expected to lead to reasonable predictions when the fibre volume fraction is small, as in a single fibre pull-out or fragmentation test, but it is expected to lead to very useful predictions for use in fibre failure or matrix cracking models applied to unidirectional composites of practical interest. It is worth noting that shear-lag predictions of stress-strain behaviour in presence of matrix cracking have been compared [McCartney (1991)] with predictions based on the more accurate stress transfer model described in [McCartney (1989)], where it was shown that shear-lag predictions significantly over estimate (by about 25%) the initial matrix cracking stress.

Stress transfer between fibre and matrix will be considered for the idealised case when either a fibre of a composite is uniformly fragmented, or when the matrix has cracked uniformly so that the matrix cracks are normal to the fibre axis. The analysis to be presented here focuses on a simplifying situation where the fibre/matrix interface is assumed to be frictionally bonded. This means that there is no bonding between fibre and matrix. It is assumed that thermal residual stresses are such that the matrix clamps the fibre so that the composite will behave as a perfectly bonded composite provide that there is no slippage between the fibre and matrix. This would certainly be the situation for an undamaged composite. If a fibre fracture or matrix crack is present then some fibre/matrix slippage is expected near the fracture plane. An indication will be given of how bonded interfaces may be analysed.

Sections 2-8 of the paper develop analytical expressions for the stress and displacement distributions in the fibre and matrix, and formulate appropriate boundary conditions for the presence of fibre fractures or matrix cracks. Section 9 solves the

stress transfer problem for the special case when there is no slip between fibre and matrix, while Section 10 extends the analysis so that sliding interfaces can be considered for which the interfacial shear stress has a uniform prescribed value that is a material characteristic. Section 11 considers an alternative stress transfer model for sliding interfaces where stress transfer in the sliding region is governed by the Coulomb friction law. Results of predictions, their discussion and conclusions are presented in Sections 12–14. Appendices A and B provide respectively solutions for the special case of an undamaged composite, and for the critical case of interface separation in a frictionally bonded composite.

2 Field equations

A set of cylindrical polar coordinates (r, θ, z) is introduced such that the origin lies on the common axis of the two concentric cylinders (with the z -axis directed along the axis of the cylinders) at the mid-point between two neighbouring fibre fractures or two neighbouring matrix cracks. Superscripts f and m will be used to denote parameters associated with the fibre and matrix respectively. For axisymmetric problems, the following equilibrium equations must be satisfied for both the fibre and matrix,

$$\frac{\partial \sigma_{rr}}{\partial r} + \frac{\partial \sigma_{rz}}{\partial z} + \frac{\sigma_{rr} - \sigma_{\theta\theta}}{r} = 0, \quad (1)$$

$$\frac{\partial \sigma_{zz}}{\partial z} + \frac{\partial \sigma_{rz}}{\partial r} + \frac{\sigma_{rz}}{r} = 0. \quad (2)$$

The fibre and matrix are regarded as transverse isotropic solids so that the relevant stress-strain-temperature relations, in terms of the axial and transverse moduli E , Poisson's ratios ν , shear modulus μ and thermal expansion coefficients α are of the form

$$\epsilon_{rr} = \frac{\partial u_r}{\partial r} = \frac{1}{E_T} \sigma_{rr} - \frac{\nu_T}{E_T} \sigma_{\theta\theta} - \frac{\nu_A}{E_A} \sigma_{zz} + \alpha_T \Delta T, \quad (3)$$

$$\epsilon_{\theta\theta} = \frac{u_r}{r} = -\frac{\nu_T}{E_T} \sigma_{rr} + \frac{1}{E_T} \sigma_{\theta\theta} - \frac{\nu_A}{E_A} \sigma_{zz} + \alpha_T \Delta T, \quad (4)$$

$$\epsilon_{zz} = \frac{\partial u_z}{\partial z} = -\frac{\nu_A}{E_A} \sigma_{rr} - \frac{\nu_A}{E_A} \sigma_{\theta\theta} + \frac{1}{E_A} \sigma_{zz} + \alpha_A \Delta T, \quad (5)$$

$$\epsilon_{rz} = \frac{1}{2} \left(\frac{\partial u_r}{\partial z} + \frac{\partial u_z}{\partial r} \right) = \frac{\sigma_{rz}}{2\mu_A}, \quad (6)$$

$$\text{where } E_T = 2\mu_T(1 + \nu_T) \text{ but } E_A \neq 2\mu_A(1 + \nu_A). \quad (7)$$

The subscripts A and T refer the properties to the axial and transverse directions relative to the direction of the fibre axis. Following Nairn (1992), when both σ_{zz} and ΔT are independent of r , the displacement u_r is compatible with the stress-strain relations (3) and (4) if the following compatibility equation for stresses is satisfied

$$(1 + \nu_T) \frac{\sigma_{rr} - \sigma_{\theta\theta}}{r} = \frac{\partial}{\partial r} (\sigma_{\theta\theta} - \nu_T \sigma_{rr}), \quad (8)$$

which is obtained by subtracting (4) from (3), differentiating (4) with respect to r , and then eliminating the displacement component u_r .

3 Interfacial and radial boundary conditions

The inner cylinder represents the fibre, which has radius R . The outer cylinder representing the matrix has radius a such that $a = R/\sqrt{V_f}$ where V_f is the volume fraction of the composite represented by the concentric cylinder model ensuring that the fibre volume fraction for the concentric cylinder model is the same as that of the composite being modelled. The volume fraction of the matrix is given by $V_m = 1 - V_f$. At the interface $r = R$ between the cylinders, the following continuity conditions must be satisfied for all values of z :

No slip region:

$$\begin{aligned} \sigma_{rr}^f(R, z) &= \sigma_{rr}^m(R, z), & \sigma_{rz}^f(R, z) &= \sigma_{rz}^m(R, z), \\ u_r^f(R, z) &= u_r^m(R, z), & u_z^f(R, z) &= u_z^m(R, z). \end{aligned} \quad (9)$$

Sliding region:

$$\begin{aligned} \sigma_{rr}^f(R, z) &= \sigma_{rr}^m(R, z), & \sigma_{rz}^f(R, z) &= \sigma_{rz}^m(R, z), \\ u_r^f(R, z) &= u_r^m(R, z), & \sigma_{rz}^f(R, z) &= \xi [\theta \tau + \varphi \eta \sigma_{rr}^f(R, z)]. \end{aligned} \quad (10)$$

In (10), τ and η are regarded as material constants where $\theta, \varphi = 0$ or 1 , and where $\xi = -1$ or $\xi = 1$. By selecting $\theta = 1$ and $\varphi = 0$ the boundary conditions (10) correspond to the those for an interface subject to a uniform interfacial shear stress $\pm\tau$. By selecting $\theta = 0$ and $\varphi = 1$ the boundary conditions correspond to those for an interface subject to the Coulomb law of friction where the parameter η is the friction coefficient. By selecting $\xi = 1$ the boundary conditions (10) correspond to those for a matrix crack, and by selecting $\xi = -1$ the conditions correspond to those for a fibre fracture. The boundary conditions (10) assume that on slipping

at the interface, the fibre and matrix remain in contact with one another and give rise to stress transfer between the cylinders where the fibre may slip relative to the matrix. If mechanical contact is lost then clearly the stress components σ_{rr} and σ_{rz} are both zero and the displacement component u_r is discontinuous across such an interface. As no stress transfer occurs at such an interface, this case will not be considered in this paper. On the external surface $r = a$ of the outer cylinder the following boundary conditions are often imposed

$$\sigma_{rr}(a, z) = \sigma_T, \quad \sigma_{rz}(a, z) = 0, \quad (11)$$

where σ_T is a uniform transverse stress applied to the external surface of the outer cylinder. In regions away from the loading mechanism, and any matrix crack or fibre fracture, it is assumed that

$$u_z^f \equiv u_z^m \equiv \varepsilon_A z, \quad (12)$$

where ε_A is the axial strain in such regions. The relation (12) is valid for all values of z when there is no fibre/matrix slippage and the system is undamaged, as described in Appendix A.

The boundary condition (11) for the radial stress could be replaced by a corresponding radial displacement condition, which would be appropriate when modelling fibre fractures embedded with a unidirectional composite, as considered in reference [Hutchinson and Jensen (1990)]. The radial component could be selected to be the radial displacement that would arise in an undamaged composite (see [McCartney (1996)] for an example of this approach). The analysis of this paper will consider only boundary conditions of the type given in (11).

4 Representation for the stress and displacement fields

The approach to developing a solution for a damaged system is to express the solution as a sum of the undamaged solution (see Appendix A) and a perturbation solution arising from the damage. For the fibre region $0 \leq r \leq R$, the stress field when damage is present is assumed to be of the following form equivalent to that assumed by Nairn (1992)

$$\sigma_{zz}^f(r, z) = \sigma_f - C(z), \quad (13)$$

$$\sigma_{rz}^f(r, z) = \frac{1}{2}C'(z)r, \quad (14)$$

$$\sigma_{rr}^f(r, z) = -\frac{1}{16}(3 + \nu_T^f)C''(z)r^2 + R_f(z) + \sigma_T - V_m \frac{\phi}{R^2}, \quad (15)$$

$$\sigma_{\theta\theta}^f = -\frac{1}{16}(1 + 3\nu_T^f)C''(z)r^2 + R_f(z) + \sigma_T - V_m \frac{\phi}{R^2}, \quad (16)$$

where σ_f and ϕ relate to the undamaged solution (see Appendix A), σ_f being the uniform axial fibre stress in an undamaged composite subject to the same loading conditions and temperature. For the matrix region $R \leq r \leq a$, the stress field is assumed to be of the following form, again equivalent to that used by Nairn (1992)

$$\sigma_{zz}^m(r, z) = \sigma_m + \frac{V_f}{V_m}C(z), \quad (17)$$

$$\sigma_{rz}^m(r, z) = \frac{C'(z)}{2V_m} \left(\frac{R^2}{r} - V_f r \right), \quad (18)$$

$$\begin{aligned} \sigma_{rr}^m(r, z) = & \left[(3 + \nu_T^m) \frac{r^2}{a^2} - 4(1 + \nu_T^m) \ln \frac{r}{a} - 2(1 - \nu_T^m) \right] \frac{R^2}{16V_m} C''(z) \\ & + R_m(z) - \frac{S_m(z)}{r^2} + \sigma_T + \phi \left(\frac{1}{a^2} - \frac{1}{r^2} \right), \end{aligned} \quad (19)$$

$$\begin{aligned} \sigma_{\theta\theta}^m(r, z) = & \left[(1 + 3\nu_T^m) \frac{r^2}{a^2} - 4(1 + \nu_T^m) \ln \frac{r}{a} + 2(1 - \nu_T^m) \right] \frac{R^2}{16V_m} C''(z) \\ & + R_m(z) + \frac{S_m(z)}{r^2} + \sigma_T + \phi \left(\frac{1}{a^2} + \frac{1}{r^2} \right), \end{aligned} \quad (20)$$

where σ_m is the uniform axial matrix stress in an undamaged composite subject to the same loading conditions and temperature (see Appendix A). It should be noted that the interface continuity relations (9)₂ and (10)₂ are satisfied by the relations (14) and (18). The functions $C(z)$ and $R_f(z)$, $R_m(z)$ and $S_m(z)$ are regarded as being identically zero when no form of damage is present and the fibre/matrix interface has not slipped.

On using (3) or (4), together with (13), (15) and (16), the corresponding representation for the displacement component u_r^f , for the fibre region $0 \leq r \leq R$, is given by

$$\frac{u_r^f(r, z)}{r} = -\frac{1 - \nu_T^f}{32\mu_T^f} C''(z)r^2 + \frac{\nu_A^f}{E_A^f} C(z) + \frac{1 - \nu_T^f}{E_T^f} R_f(z) + A_f, \quad (21)$$

where A_f is defined in Appendix A. On using (6), (14) and (21) it can be shown on

integrating with respect to r that for $0 \leq r \leq R$,

$$u_z^f(r, z) = -\frac{1}{2} \left[\left(\frac{\nu_A^f}{E_A^f} - \frac{1}{2\mu_A^f} \right) C'(z) + \frac{1 - \nu_T^f}{E_T^f} R_f'(z) \right] (r^2 - R^2) + \frac{1 - \nu_T^f}{128\mu_T^f} C'''(z)(r^4 - R^4) + H_f(z) + \epsilon_A z, \tag{22}$$

where $H_f(z) + \epsilon z \equiv u_z^f(R, z)$ arises from the integration representing the axial displacement distribution in the fibre along the interface. The function $H_f(z) \equiv 0$ when the system is in an undamaged state. Similarly, the corresponding displacement components for the matrix region $R \leq r \leq a$ are given by

$$\frac{u_r^m(r, z)}{r} = \left(\frac{1}{2} \frac{r^2}{a^2} - 2 \ln \frac{r}{a} + 1 \right) \frac{1 - \nu_T^m R^2}{16\mu_T^m V_m} C''(z) - \frac{\nu_A^m V_f}{E_A^m V_m} C(z) + \frac{1 - \nu_T^m}{E_T^m} R_m(z) + \frac{S_m(z)}{2\mu_T^m r^2} + A_m + \frac{\phi}{2\mu_T^m r^2}, \tag{23}$$

$$u_z^m(r, z) = \frac{1 - \nu_T^m R^2}{16\mu_T^m V_m} C'''(z) r^2 \ln \frac{r}{R} + \left(\frac{R^2}{2\mu_A^m V_m} C'(z) - \frac{S_m'(z)}{2\mu_T^m} \right) \ln \frac{r}{R} + \frac{1}{2} \left[\left(\frac{\nu_A^m}{E_A^m} - \frac{1}{2\mu_A^m} \right) \frac{V_f}{V_m} C'(z) - \frac{1 - \nu_T^m}{16\mu_T^m} \frac{2 - \ln V_f}{V_m} R^2 C'''(z) - \frac{1 - \nu_T^m}{E_T^m} R_m'(z) \right] (r^2 - R^2) - \frac{1 - \nu_T^m}{128\mu_T^m} \frac{V_f}{V_m} C'''(z)(r^4 - R^4) + H_m(z) + \epsilon_A z, \tag{24}$$

where A_m is defined in Appendix A and where $H_m(z) + \epsilon z \equiv u_z^m(R, z)$ arises from the integration representing the axial displacement distribution in the matrix along the interface. The function $H_m(z) \equiv 0$ when the system is in an undamaged state. It should be noted that the displacement component u_θ is everywhere zero in both the fibre and matrix.

The stress and displacement fields specified by (13)-(24) satisfy exactly the equilibrium equations, and the compatibility equations together with the stress-strain relations (3), (4) and (6) for any function $C(z)$, and for any functions $R_f(z)$, $R_m(z)$, $S_m(z)$, $H_f(z)$ and $H_m(z)$. In addition, the function $C'(z)$ is double the value of the interfacial shear stress σ_{rz} at the point z , and since from (11)₂ $\sigma_{rz}(a, z) \equiv 0$ it follows from (13), (17) and A22 that

$$V_f \sigma_{zz}^f(r, z) + V_m \sigma_{zz}^m(r, z) = \sigma_A, \tag{25}$$

for all values of r and z . It should be noted that the axial stress-strain equation (5) will be considered in Section 6.

5 Determination of the integration functions

The next objective is to determine the functions $R_f(z)$, $R_m(z)$ and $S_m(z)$ that were introduced when carrying out integrations of the equilibrium equations in terms of the stress-transfer function $C(z)$. The application of the external boundary condition (11)₁ for the radial stress to the relation (19) leads to the following expression for the function $S_m(z)$

$$\frac{S_m(z)}{a^2} = (1 + 3\nu_T^m) \frac{R^2}{16V_m} C''(z) + R_m(z). \quad (26)$$

The application of the interfacial continuity condition (9)₁ or (10)₁ for the radial stress using (15), (19) and (26) leads to the relation

$$V_f R_f(z) + V_m R_m(z) = \alpha R^2 C''(z), \quad (27)$$

where

$$\alpha = \frac{1}{16} \left(V_f \nu_T^f + V_m \nu_T^m - (1 + 4\nu_T^m) - 2(1 + \nu_T^m) \frac{V_f}{V_m} \ln V_f \right). \quad (28)$$

The application of the interfacial continuity condition (9)₃ or (10)₃ for the radial displacement using (7), (21), (23), (26), and the relations (A8) and (A9) for an undamaged composite, leads to the relation

$$\left(\frac{\nu_A^f}{E_A^f} + \frac{\nu_A^m V_f}{E_A^m V_m} \right) C(z) - \left[(1 - \nu_T^f) \frac{\mu_T^m}{\mu_T^f} + (1 - \nu_T^m) \frac{V_f + 2(1 - \ln V_f)}{V_m} \right. \\ \left. + \frac{1 + 3\nu_T^m}{V_f V_m} \right] \frac{R^2 C''(z)}{32\mu_T^m} + \frac{1 - \nu_T^f}{1 + \nu_T^f} \frac{R_f(z)}{2\mu_T^f} - \left(\frac{1 - \nu_T^m}{1 + \nu_T^m} + \frac{1}{V_f} \right) \frac{R_m(z)}{2\mu_T^m} = 0. \quad (29)$$

The equations (27) and (29) are then solved simultaneously for the functions $R_f(z)$ and $R_m(z)$ so that

$$R_m(z) = \beta C(z) + \gamma R^2 C''(z), \\ R_f(z) = -\beta \frac{V_m}{V_f} C(z) + \frac{1}{V_f} (\alpha - \gamma V_m) R^2 C''(z), \quad (30)$$

where

$$\beta = 2\mu_T^m V_f \left(\frac{v_A^f}{V_f E_A^f} + \frac{v_A^m}{V_m E_A^m} \right) \omega,$$

$$\gamma = \left[\frac{1 - v_T^f \mu_T^m}{1 + v_T^f \mu_T^f} \left(\frac{\alpha}{V_f} - \frac{1 + v_T^f}{16} \right) - (1 - v_T^m) \frac{V_f + 2(1 - \ln V_f)}{16V_m} - \frac{1 + 3v_T^m}{16V_f V_m} \right] \omega, \tag{31}$$

$$\frac{1}{\omega} = \frac{1 - v_T^f \mu_T^m V_m}{1 + v_T^f \mu_T^f V_f} + \frac{1 - v_T^m}{1 + v_T^m} + \frac{1}{V_f}.$$

6 Derivation of differential equation for stress transfer before interface slip-page

For the stress and displacement representations derived above it is not possible to satisfy exactly the stress-strain relations for the fibre and matrix having the form given by (5). However, it is possible to satisfy corresponding averaged stress-strain relations. For the fibre the averaged stress-strain relation is

$$\frac{d\bar{u}_z^f}{dz} = -\frac{v_A^f}{E_A^f} (\bar{\sigma}_{rr}^f + \bar{\sigma}_{\theta\theta}^f) + \frac{\bar{\sigma}_{zz}^f}{E_A^f} + \alpha_A^f \Delta T, \tag{32}$$

where an average value is denoted by an overbar and defined for any function $f(r, z)$ associated with the fibre by

$$\pi R^2 \bar{f}(z) \equiv \int_0^R 2\pi r f(r, z) dr. \tag{33}$$

On averaging (22) using (33), it can be shown that

$$\bar{u}_z^f(z) = -\frac{1 - v_T^f}{192\mu_T^f} R^4 C'''(z) + \frac{R^2}{4} \left[\frac{1 - v_T^f}{E_T^f} R_f'(z) + \left(\frac{v_A^f}{E_A^f} - \frac{1}{2\mu_A^f} \right) C'(z) \right] + H_f(z) + \varepsilon z. \tag{34}$$

For the matrix the averaged stress-strain relation is

$$\frac{d\bar{u}_z^m}{dz} = -\frac{v_A^m}{E_A^m} (\bar{\sigma}_{rr}^m + \bar{\sigma}_{\theta\theta}^m) + \frac{\bar{\sigma}_{zz}^m}{E_A^m} + \alpha_A^m \Delta T, \tag{35}$$

where an average value is denoted by an overbar and defined for any function $m(r, z)$ associated with the matrix by

$$\pi(a^2 - R^2)\bar{m}(z) \equiv \int_R^a 2\pi r m(r, z) dr. \quad (36)$$

On averaging (24) using (36), it can be shown that

$$\begin{aligned} \bar{u}_z^m(z) = & a_m \frac{1 - \nu_T^m R^2}{16\mu_T^m V_m} C'''(z) + b_m \left(\frac{R^2}{2\mu_A^m V_m} C'(z) - \frac{S'_m(z)}{2\mu_T^m} \right) - c_m \frac{1 - \nu_T^m V_f}{128\mu_T^m V_m} C'''(z) \\ & + \frac{d_m}{2} \left[\left(\frac{\nu_A^m}{E_A^m} - \frac{1}{2\mu_A^m} \right) \frac{V_f}{V_m} C'(z) - \frac{1 - \nu_T^m}{16\mu_T^m} \frac{2 - \ln V_f}{V_m} R^2 C'''(z) - \frac{1 - \nu_T^m}{E_T^m} R'_m(z) \right] \\ & + H_m(z) + \varepsilon_{AZ}, \end{aligned} \quad (37)$$

where

$$\begin{aligned} a_m &= \frac{1}{a^2 - R^2} \int_R^a 2r^3 \ln \frac{r}{R} dr = \frac{1}{8(a^2 - R^2)} \left(4a^4 \ln \frac{a}{R} + R^4 - a^4 \right) \\ &= \frac{R^2}{8V_f V_m} (V_f^2 - 1 - 2 \ln V_f), \\ b_m &= \frac{1}{a^2 - R^2} \int_R^a 2r \ln \frac{r}{R} dr = \frac{1}{2(a^2 - R^2)} \left(2a^2 \ln \frac{a}{R} + R^2 - a^2 \right) = -\frac{1}{2} \left(1 + \frac{1}{V_m} \ln V_f \right), \end{aligned} \quad (38)$$

$$c_m = \frac{1}{a^2 - R^2} \int_R^a 2r(r^4 - R^4) dr = \frac{1}{3}(a^2 - R^2)(a^2 + 2R^2) = \frac{R^4 V_m (1 + 2V_f)}{3 V_f^2},$$

$$d_m = \frac{1}{a^2 - R^2} \int_R^a 2r(r^2 - R^2) dr = \frac{1}{2}(a^2 - R^2) = \frac{R^2 V_m}{2 V_f}.$$

On averaging (15) and (16) using (33), and on averaging (19) and (20) using (36), it can be shown that

$$\bar{\sigma}_{rr}^f(z) + \bar{\sigma}_{\theta\theta}^f(z) = 2 \left(\frac{\alpha}{V_f} - \frac{V_m}{V_f} \gamma - \frac{1 + \nu_T^f}{16} \right) R^2 C''(z) - 2\beta \frac{V_m}{V_f} C(z) + 2 \left(\sigma_T - V_m \frac{\phi}{R^2} \right), \quad (39)$$

$$\bar{\sigma}_{rr}^m(z) + \bar{\sigma}_{\theta\theta}^m(z) = \left[2\gamma + \frac{1 + \nu_T^m}{8V_m^2} \{ (3 + V_f)V_m + 2V_f \ln V_f \} \right] R^2 C''(z) + 2\beta C(z) + 2 \left(\sigma_T + V_f \frac{\phi}{R^2} \right). \tag{40}$$

For an unslipped interface, the identification $H_f(z) \equiv H_m(z) \equiv H(z)$ is made in order to satisfy the boundary condition (9)₄. The substitution of (13), (34) and (39) in (32), and of (17), (37) and (40) in (35), followed by a subtraction to eliminate the function $H(z)$, leads to the following homogeneous fourth order ordinary differential equation that must be satisfied by the stress transfer function $C(z)$ in the unslipped region

$$FR^4 C''''(z) + GR^2 C''(z) + HC(z) = 0, \tag{41}$$

where the constant coefficients F , G and H are given by

$$\begin{aligned} F &= F_0 + \alpha F_\alpha + \beta F_\beta + \gamma F_\gamma, \\ G &= G_0 + \alpha G_\alpha + \beta G_\beta + \gamma G_\gamma, \\ H &= H_0 + \alpha H_\alpha + \beta H_\beta + \gamma H_\gamma, \end{aligned} \tag{42}$$

where the parameters $F_0, F_\alpha, F_\beta, F_\gamma$ etc. are given by

$$\begin{aligned} F_0 &= \frac{(\nu_T^m)^2}{192V_f V_m^2 E_T^m} [V_m(V_f^2 + 4V_f - 17) - 3(1 + V_f)(3 - V_f) \ln V_f] \\ &\quad - \frac{\nu_T^m}{16V_f V_m^2 E_T^m} (V_m + \ln V_f) + \frac{1}{192V_f E_T^m} (5 + V_f - 3 \ln V_f) - \frac{1 - (\nu_T^f)^2}{192E_T^f}, \end{aligned} \tag{43}$$

$$F_\alpha = \frac{1 - \nu_T^f}{8V_f E_T^f}, F_\beta = 0, F_\gamma = -\frac{1 + \nu_T^m}{8V_f V_m E_T^m} [(1 + V_f)V_m + 2 \ln V_f] - \frac{\nu_T^m}{4E_T^m} \frac{V_m}{V_f} - \frac{1 - \nu_T^f}{8E_T^f} \frac{V_m}{V_f},$$

$$\begin{aligned} G_0 &= \frac{1}{16V_m^2 \mu_A^m} [(3 - V_f)V_m + 2 \ln V_f] - \frac{1}{16\mu_A^f} - \frac{\nu_A^m}{8E_A^m} \\ &\quad - \frac{\nu_A^m(1 + \nu_T^m)}{16V_m^2 E_A^m} [(3 + V_f)V_m + 2V_f \ln V_f] + \frac{\nu_A^f(1 - \nu_T^f)}{16E_A^f}, \end{aligned} \tag{44}$$

$$G_\alpha = \frac{\nu_A^f}{V_f E_A^f}, G_\beta = F_\gamma, G_\gamma = -V_m \left(\frac{\nu_A^f}{V_f E_A^f} + \frac{\nu_A^m}{V_m E_A^m} \right),$$

$$H_0 = \frac{V_f}{2} \left(\frac{1}{V_f E_A^f} + \frac{1}{V_m E_A^m} \right), H_\alpha = 0, H_\beta = G_\gamma, H_\gamma = 0. \tag{45}$$

It has been shown using the algebraic programming language REDUCE, that F , G and H correspond to formulae given by Nairn (1992) derived using a variational technique (N.B. the expression for C_{35} given by Nairn should include a minus sign before the ratio $(V_2A_1)/(V_1A_2)$ that appears in his result). It is concluded that the approach being taken provides the displacement field corresponding to the stress-based variational calculation [Nairn (1992)] that minimises the complementary energy.

7 The average axial displacement functions

The substitution of (13), (17), (39) and (40) in (32) and (35), followed by an integration with respect to z leads to the following expressions for the averages of the axial displacement components in the fibre and matrix respectively

$$\bar{u}_z^f(z) = -\frac{2v_A^f}{E_A^f} \left(\frac{\alpha}{V_f} - \frac{V_m}{V_f} \gamma - \frac{1+v_T^f}{16} \right) R^2 C'(z) - \frac{1}{E_A^f} \left(1 - 2\beta v_A^f \frac{V_m}{V_f} \right) \bar{C}(z) + \varepsilon_A z, \quad (46)$$

$$\begin{aligned} \bar{u}_z^m(z) = & -\frac{2v_A^m}{E_A^m} \left[\gamma + \frac{1+v_T^m}{16V_m^2} \{ (3+V_f)V_m + 2V_f \ln V_f \} \right] R^2 C'(z) \\ & + \frac{V_f}{V_m E_A^m} \left(1 - 2\beta v_A^m \frac{V_m}{V_f} \right) \bar{C}(z) + \varepsilon_A z, \end{aligned} \quad (47)$$

where

$$\bar{C}(z) = \int_0^z C(z') dz'. \quad (48)$$

The only remaining functions that have not been determined are the integration functions $H_f(z)$ and $H_m(z)$ appearing in the relations (22) and (24) for the axial displacement in fibre and matrix respectively. The function $H_f(z)$ is obtained using the equivalent results (34) and (46) so that

$$\begin{aligned} H_f(z) = & -\frac{1-v_T^f}{4E_T^f} \left(\frac{\alpha}{V_f} - \frac{V_m}{V_f} \gamma - \frac{1+v_T^f}{24} \right) R^4 C'''(z) + \left(\frac{1-v_T^f}{4E_T^f} \frac{V_m}{V_f} \beta + \frac{1}{8\mu_A^f} \right) R^2 C'(z) \\ & - \frac{2v_A^f}{E_A^f} \left(\frac{\alpha}{V_f} - \frac{V_m}{V_f} \gamma + \frac{1+v_T^f}{16} \right) R^2 C'(z) - \frac{1}{E_A^f} \left(1 - 2\beta v_A^f \frac{V_m}{V_f} \right) \bar{C}(z). \end{aligned} \quad (49)$$

The function $H_m(z)$ is obtained using the equivalent results (37) and (47) so that

$$\begin{aligned}
 H_m(z) = & \frac{R^4 C'''(z)}{96V_f V_m^2 E_T^m} [V_m^2(5 + V_f) - 12v_T^m V_m + (v_T^m)^2 V_m \{V_f^2 + 4V_f - 17\}] \\
 & - \frac{R^4 C'''(z)}{32V_f V_m^2 E_T^m} [V_m^2 + 4v_T^m + (v_T^m)^2(1 + V_f)(3 - V_f)] \ln V_f \\
 & - \frac{\gamma R^4 C'''(z) + \beta R^2 C'(z)}{4V_f V_m E_T^m} [V_m \{1 + V_f + v_T^m(3 - V_f)\} + 2(1 + v_T^m) \ln V_f] \\
 & - \frac{v_A^m R^2 C'(z)}{8V_m^2 E_A^m} [V_m \{5 - V_f + v_T^m(3 + V_f)\} + 2(1 + v_T^m) V_f \ln V_f + 16\gamma V_m^2] \\
 & + \frac{R^2 C'(z)}{8V_m^2 \mu_A^m} [V_m(3 - V_f) + 2 \ln V_f] + \frac{V_f}{V_m E_A^m} \left(1 - 2\beta v_A^m \frac{V_m}{V_f} \right) \bar{C}(z). \quad (50)
 \end{aligned}$$

In the absence of sliding, when

$$H_f(z) \equiv H_m(z) \equiv H(z) \text{ and } u_z^f(R, z) \equiv u_z^m(R, z),$$

the solution for the stress and displacement fields in the fibre and matrix derived in Section 5 satisfy exactly the equilibrium equations (1) and (2), the stress-strain relations (3), (4) and (6), the compatibility equation (8), the interface conditions (9) and the external boundary conditions (11) for any stress transfer function $C(z)$. The stress and displacement fields do not satisfy the axial stress-strain relation (5), but they do satisfy exactly the corresponding averaged stress-strain relations (32) and (35) provided that the stress transfer function $C(z)$ satisfies the homogeneous fourth order ordinary differential equation (41). If the interface is sliding, then $H_f(z) \neq H_m(z)$ and consequently neither the differential equation (41) nor the interface condition (9)₄ are satisfied, although the relations (49) and (50) remain valid.

8 Axial boundary conditions

A length $2L$ of fibre and matrix are now considered where the origin of the (r, z) coordinates is at the centre of the system on the axis of the fibre. On $z = \pm L$, there are either fibre fractures or matrix cracks, and the shear stress σ_{rz} is assumed to be everywhere zero, so that the solution to the problem can be applied to the fibre fragmentation and matrix cracking problems for the special case where the crack distribution is uniform in either the fibre or the matrix. It then follows from (14) and (18) that this shear stress boundary condition is satisfied if $C'(\pm L) = 0$.

The boundary condition for the axial stress is written in the following generalised

form that can be used for fibre fractures or matrix cracks

$$\begin{aligned}\sigma_{zz}^f(r, \pm L) &= \frac{(1 + \xi)\sigma_A}{2V_f}, 0 \leq r \leq R, \\ \sigma_{zz}^m(r, \pm L) &= \frac{(1 - \xi)\sigma_A}{2V_m}, R \leq r \leq a,\end{aligned}\quad (51)$$

where σ_A is the effective axial applied stress. It is clear that these values are consistent with the relation (25). On setting $\xi = -1$, the boundary conditions (51) are valid for fibre fractures, and on setting $\xi = 1$ these boundary conditions are valid for matrix cracks. On using (13) and (17), the boundary conditions (51) lead to the condition

$$C(\pm L) = \sigma_f - \frac{(1 + \xi)\sigma_A}{2V_f} = \frac{(1 - \xi)\sigma_A}{2V_f} - \frac{V_m}{V_f}\sigma_m = F(\sigma_A, \sigma_T, \Delta T), \quad (52)$$

where σ_f and σ_m are the uniform axial fibre and matrix stresses for an undamaged composite. The function F depends linearly on σ_A , σ_T and ΔT , as seen from (A12), (A18), (A21) and (A23). To determine values of F , the effective properties E_A , ν_A and α_A are first calculated using (A24)-(A29). Given values of σ_A , σ_T and ΔT , the axial strain ϵ_A is first calculated using (A23) and then the parameters ϕ , σ_f and σ_m using (A12), (A18) and (A21). The value of σ_f or σ_m is then substituted into (52) to calculate $C(\pm L) = F(\sigma_A, \sigma_T, \Delta T)$.

9 Isolated fractures in the absence of interface sliding

Consider now an isolated fibre fracture or matrix crack located at $z = L$, where the interface has not slipped, as illustrated in Fig. 1.

It is convenient to express the solution of the ordinary differential equation (41) in the following form (valid for $0 \leq z \leq L$)

$$C(z) = A \cosh \frac{(p+q)z}{R} + B \cosh \frac{(p-q)z}{R}, \quad (53)$$

where

$$p = \sqrt{\frac{1}{2}(r+s)}, \quad q = \sqrt{\frac{1}{2}(r-s)} < p, \quad r = -\frac{G}{2F} > 0, \quad s = \sqrt{\frac{H}{F}}. \quad (54)$$

The form of solution given by (53) is valid only if $r > s$, a situation which is often encountered when applying the model to common composites having volume fractions which are not too large. The situation $r < s$ leads to complex values of q . The

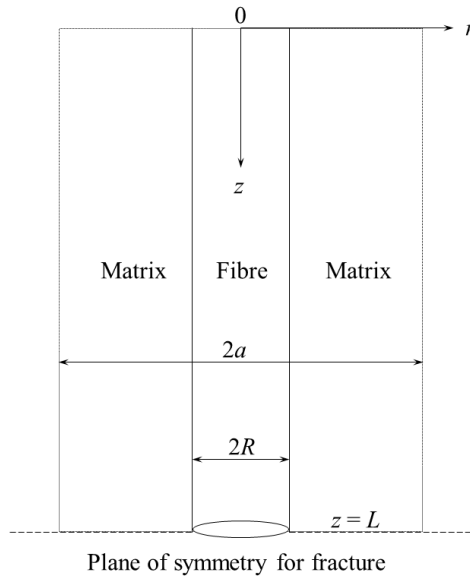


Figure 1: Schematic diagram showing the geometry for an unslipped interface associated with a fibre fracture or matrix crack.

easiest way of dealing with this case is to develop computer code using complex arithmetic for variables that will be complex numbers. It should be noted that p is always real and that the situation $r = s$ needs to be considered as a special case when writing software.

In (53), the parameters A and B are to be determined using the boundary conditions $C'(\pm L) = 0$ and (52). It can be shown that

$$A = -\frac{(p - q) \tanh \frac{(p - q)L}{R}}{\cosh \frac{(p + q)L}{R}} \Lambda F(\sigma_A, \sigma_T, \Delta T), B = \frac{(p + q) \tanh \frac{(p + q)L}{R}}{\cosh \frac{(p - q)L}{R}} \Lambda F(\sigma_A, \sigma_T, \Delta T), \tag{55}$$

where

$$\frac{1}{\Lambda} = (p + q) \tanh \frac{(p + q)L}{R} - (p - q) \tanh \frac{(p - q)L}{R}, \tag{56}$$

and where the function F is defined by (52). The stress transfer function, for an array of equally spaced interacting cracks in the fibre or matrix before interface sliding occurs, is thus determined uniquely.

The distribution of the interfacial shear stress is obtained by substituting (53) in (14) or (18). The interfacial shear stress will be zero at the location of the crack $z = L$, and the maximum absolute value of the interfacial shear stress occurs when $C''(z) = 0$ defining the point $z = c$ for a local maximum or minimum of the interfacial shear stress. It follows from (53) that the value of c must be such that

$$(p+q)^2 A \cosh \frac{(p+q)c}{R} + (p-q)^2 B \cosh \frac{(p-q)c}{R} = 0. \quad (57)$$

When $r > s$ so that q is a real quantity, it can be shown that the parameter c satisfies the following transcendental equation that is solved numerically

$$\tanh \frac{pc}{R} \tanh \frac{qc}{R} = \frac{p \tanh \frac{qL}{R} - q \tanh \frac{pL}{R}}{p \tanh \frac{pL}{R} - q \tanh \frac{qL}{R}}. \quad (58)$$

While the relation (58) is compact, it might cause numerical problems when q is a pure imaginary number as the \tanh functions would be replaced by \tan functions which periodically diverge. To avoid this potential problem, the relation (58) is expressed in the following more expansive form that avoids the need to evaluate \tanh functions

$$\begin{aligned} & \sinh \frac{pc}{R} \sinh \frac{qc}{R} \left(p \sinh \frac{pL}{R} \cosh \frac{qL}{R} - q \cosh \frac{pL}{R} \sinh \frac{qL}{R} \right) \\ & = \cosh \frac{pc}{R} \cosh \frac{qc}{R} \left(p \cosh \frac{pL}{R} \sinh \frac{qL}{R} - q \sinh \frac{pL}{R} \cosh \frac{qL}{R} \right). \end{aligned} \quad (59)$$

The value $\bar{\tau}$ of the local maximum or minimum interfacial shear stress is obtained using (14) and (53) so that

$$\bar{\tau} = \frac{1}{2} A (p+q) \sinh \frac{(p+q)c}{R} + \frac{1}{2} B (p-q) \sinh \frac{(p-q)c}{R}. \quad (60)$$

On using (55)

$$\bar{\tau} = \Lambda' F(\sigma_A, \sigma_T, \Delta T), \quad (61)$$

where

$$\Lambda' = \frac{p+q}{2} \tanh \frac{(p-q)L}{R} \frac{\cosh \frac{(p+q)c}{R}}{\cosh \frac{(p+q)L}{R}} \Psi(c) \Lambda, \quad (62)$$

and

$$\Psi(x) \equiv (p+q) \tanh \frac{(p-q)x}{R} - (p-q) \tanh \frac{(p+q)x}{R}. \quad (63)$$

It is worth noting that when $r < s$, so that q is a pure imaginary quantity, the transcendental equation determining the location $z = c$ is

$$\tanh \frac{pc}{R} \tan \frac{|q|c}{R} = \frac{p \tanh \frac{|q|L}{R} - |q| \tanh \frac{pL}{R}}{p \tanh \frac{pL}{R} + |q| \tanh \frac{|q|L}{R}}. \quad (64)$$

For the special case of non-interacting cracks, the interfacial shear stress will be zero at the location of the crack $z = L$, and it will tend to zero far away from the crack location. It can be shown for this special case that the maximum absolute value of the interfacial shear stress occurs at the point $z = c$ where

$$\frac{c}{L} = 1 - \frac{R}{2Lq} \ln \frac{p+q}{p-q}. \quad (65)$$

The corresponding local maximum or minimum value of the interfacial shear stress is given by

$$\bar{\tau} = \frac{1}{2} \sqrt{p^2 - q^2} \left(\frac{p+q}{p-q} \right)^{-\frac{p}{2q}} F(\sigma_A, \sigma_T, \Delta T). \quad (66)$$

10 Frictionally slipping interfaces with uniform interfacial shear stress

Consider now the situation where the fibre and matrix have slipped relative to each other along the interface such that they remain in contact and are subject to frictional slip. During progressive axial loading the transverse applied stress σ_T is assumed to be held fixed. The first case to be considered assumes that frictional slip is characterised by a uniform interfacial shear stress τ , which is regarded as a material constant. From (14) or (18) the stress transfer function in the slip zone satisfies the first order differential equation

$$C'(z) = \frac{2\tau}{R}. \quad (67)$$

The derivative $C'(z)$ governing the interfacial shear stress $\sigma_{rz}(R, z)$ is a negative quantity when stress transfer for a matrix crack ($\xi = 1$) is being analysed, but it is a positive quantity when considering stress transfer associated with a fibre fracture ($\xi = -1$). The sign of τ is set in software, selecting a negative value for matrix cracks and a positive value for fibre fractures.

Consider the geometry of the fibre, matrix and sliding interface shown in Fig. 2. The fibre has radius R and there is a fibre fracture or matrix crack at the location $z = L$. As soon as sliding is initiated at the point $z = c$ on the interface at $r = R$,

the solution of the stress transfer problem is no longer governed by the differential equation (41) alone. The differential equation applies only in the region $0 \leq z \leq b$ where elastic stress transfer is possible as the interface has not slipped in this region. For the sliding region $b \leq z \leq c$, the interfacial shear stress is assumed to have a uniform value denoted by τ . If the parameter $c = L$ then the symmetry of the stress tensor asserts that the shear stress would have the non-zero value τ on the surface of the fibre fracture or matrix crack. This situation violates the essential condition that crack surfaces should be stress-free. To overcome this problem a transition zone is introduced in the sliding zone occupying the region $c \leq z \leq L$ in which the interfacial shear stress reduces from the specified value τ at $z = c$ to zero value on $z = L$. Fibre/matrix stress transfer will be occurring in this region, as well as in the uniform shear stress zone $b \leq z \leq c$.

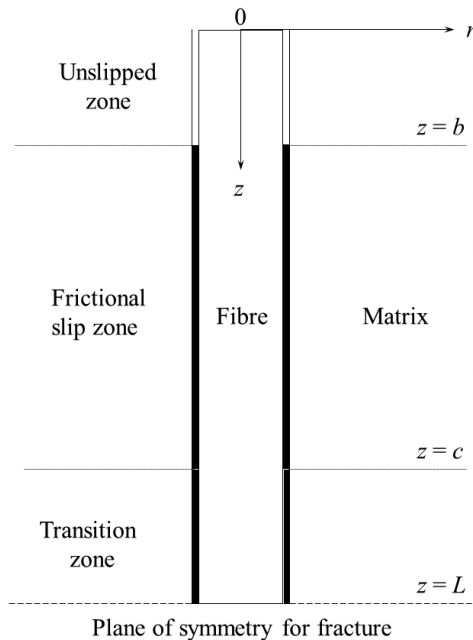


Figure 2: Schematic diagram showing the geometry for a sliding interface associated with a fibre fracture or matrix crack when the shear stress is uniform in the slipping zone.

For a fibre fracture on $z = L$ it is assumed that in the transition region the stress distribution in the fibre is identical to that which would arise for an interface that is at the point of first slipping. The stress distribution in the matrix would, however, be different. If the matrix were cracked on $z = L$ instead of the fibre, then the

stress distribution in the matrix would then be assumed to be identical to that for an interface at the point of first slipping while that in the fibre would be different. It is likely that other transition functions could be developed but this task is beyond the scope of this paper.

The representation for the stress and displacement fields defined in Section 4 apply to all three stress transfer regions shown in Fig. 2. For frictionally bonded composites the stress transfer function $C(z)$, which is used for a slipping interface having a uniform shear stress, is required to be continuous and have continuous first and second derivatives so that the axial and shear stress, and the radial displacement are continuous. For a perfectly bonded interface, a debond length would be assumed to be specified in advance, and the continuity condition for the second derivative of the function $C(z)$ would need to be relaxed (a situation not considered here).

Consider now the stress transfer function $C(z)$ for frictionally bonded interfaces having the following form

For $0 \leq z \leq b$

$$C(z) = A^* \cosh \frac{(p+q)z}{R} + B^* \cosh \frac{(p-q)z}{R}, \quad (68)$$

For $b \leq z \leq c$

$$C(z) = \frac{2\tau}{R}(z-c) + C_0 + F(\sigma_A, \sigma_T, \Delta T) - F(\sigma_A^s, \sigma_T, \Delta T), \quad (69)$$

For $c \leq z \leq L$

$$C(z) = A \cosh \frac{(p+q)z}{R} + B \cosh \frac{(p-q)z}{R} + F(\sigma_A, \sigma_T, \Delta T) - F(\sigma_A^s, \sigma_T, \Delta T). \quad (70)$$

In (69) and (70) the value of c is determined by the transcendental equation (58) and the function F is defined by (52). It is clear, from the analysis given in Section 9, that (68) satisfies the differential equation (41) for a perfectly bonded/unslipped interface. Also, it can be shown that (69) is such that the expressions (14) and (18) for the shear stress lead to the required uniform value τ on the interface $r = R$. The expression on the R.H.S. of (70) is just one possible transition function enabling the shear stress to reduce to zero at $z = L$, thus leading to matrix cracks or fibre fractures that have a zero shear traction distribution. Given a value of the interfacial shear stress τ , it follows from (61) that the initial sliding stress σ_A^s must satisfy the relation

$$\tau = \Lambda' F(\sigma_A^s, \sigma_T, \Delta T), \quad (71)$$

where the value of Λ' is given by (62).

Consider first of all the boundary conditions at the end location $z = L$. The constants A and B are selected so that

$$A \cosh \frac{(p+q)L}{R} + B \cosh \frac{(p-q)L}{R} = F(\sigma_A^s, \sigma_T, \Delta T), \quad (72)$$

$$(p+q)A \sinh \frac{(p+q)L}{R} + (p-q)B \sinh \frac{(p-q)L}{R} = 0. \quad (73)$$

The stress transfer function then satisfies the conditions $C(L) = F(\sigma_A, \sigma_T, \Delta T)$ and $C'(L) = 0$. Consistent with (55), the values of A and B are given by

$$A = -\frac{(p-q) \tanh \frac{(p-q)L}{R}}{\cosh \frac{(p+q)L}{R}} \Lambda F(\sigma_A^s, \sigma_T, \Delta T), B = \frac{(p+q) \tanh \frac{(p+q)L}{R}}{\cosh \frac{(p-q)L}{R}} \Lambda F(\sigma_A^s, \sigma_T, \Delta T). \quad (74)$$

On using (57), (62) and (71) it can be shown that

$$A = -\frac{p-q}{p+q} \frac{2\tau}{\Psi(c) \cosh \frac{(p+q)c}{R}}, B = \frac{p+q}{p-q} \frac{2\tau}{\Psi(c) \cosh \frac{(p-q)c}{R}}. \quad (75)$$

Consider now the continuity of the behaviour of the function $C(z)$ at the known location $z = c$. The continuity of $C(z)$ is assured only if the constant C_0 appearing in (69) is selected so that

$$C_0 = A \cosh \frac{(p+q)c}{R} + B \cosh \frac{(p-q)c}{R}. \quad (76)$$

On using (75) it can be shown that

$$C_0 = \frac{8pq}{p^2 - q^2} \frac{\tau}{\Psi(c)}. \quad (77)$$

The derivative $C'(z)$ must also be continuous at $z = c$, a condition that is satisfied if

$$A(p+q) \sinh \frac{(p+q)c}{R} + B(p-q) \sinh \frac{(p-q)c}{R} = 2\tau. \quad (78)$$

This condition is automatically satisfied because of the relation (60). Also the relation (57) implies that $C''(z)$ is continuous at $z = c$ having the value zero. It has thus been shown that $C(z)$, $C'(z)$ and $C''(z)$ are all continuous at $z = c$.

Consider finally the properties of the stress transfer function $C(z)$ in the unslipped region at the point $z = b$ which is as yet an unknown quantity that determines the location of the interface between the unslipped and sliding regions. There are three unknowns, namely A^* , B^* and the value of b . For consistency with the situation imposed at the point $z = c$ it is useful to apply the following conditions that ensure the continuity of $C(z)$, $C'(z)$ and $C''(z)$ at the point $z = b$. It is clear from (68) and (69) that the conditions to be satisfied are

$$\begin{aligned} A^* \cosh \frac{(p+q)b}{R} + B^* \cosh \frac{(p-q)b}{R} \\ = \frac{2\tau}{R}(b-c) + C_0 + F(\sigma_A, \sigma_T, \Delta T) - F(\sigma_A^s, \sigma_T, \Delta T), \end{aligned} \quad (79)$$

$$(p+q)A^* \sinh \frac{(p+q)b}{R} + (p-q)B^* \sinh \frac{(p-q)b}{R} = \frac{2\tau}{R}, \quad (80)$$

$$(p+q)^2 A^* \cosh \frac{(p+q)b}{R} + (p-q)^2 B^* \cosh \frac{(p-q)b}{R} = 0. \quad (81)$$

The easiest approach is to use the conditions (80) and (81), ensuring that $RC'(b) = 2\tau$, and $C''(b) = 0$, to determine the parameters A^* and B^* , with the result that

$$A^* = -\frac{p-q}{p+q} \frac{2\tau}{\Psi(b) \cosh \frac{(p+q)b}{R}}, B^* = \frac{p+q}{p-q} \frac{2\tau}{\Psi(b) \cosh \frac{(p-q)b}{R}}, \quad (82)$$

where the function Ψ is defined by (63). The values given by (82) ensure the continuity of $C'(z)$ and $C''(z)$ at $z = b$. It should be noted from (75) and (82) that when $b = c$ it follows that $A = A^*$ and $B = B^*$ recovering the distribution derived in Section 9.

The parameter b defining the location of the boundary between the unslipped and sliding zones has not yet been specified. Its value is determined by imposing the continuity of $C(z)$ at $z = b$. It can be shown from (77), (79) and (82) and that the value of b must be chosen so that

$$\left[\frac{4pq}{p^2 - q^2} \left(\frac{1}{\Psi(b)} - \frac{1}{\Psi(c)} \right) - \frac{b-c}{R} \right] 2\tau = F(\sigma_A, \sigma_T, \Delta T) - F(\sigma_A^s, \sigma_T, \Delta T). \quad (83)$$

This result, when used in conjunction with (52), shows that the length of the zone having a uniform interfacial shear stress τ is determined by the value of the stress increase from the point of sliding initiation. From (83) it is clearly seen that $b = c$ when $\sigma_A = \sigma_A^s$. The result (83) is a transcendental equation that must be solved numerically.

It is also worth noting that when $(p - q)b/R \gg 1$ there is negligible interaction of neighbouring cracks so that

$$\tanh \frac{(p - q)b}{R} \cong \tanh \frac{(p + q)b}{R} \cong 1, \text{ and } \Psi(x) \cong 2q. \quad (84)$$

The relation (83) determining the value of b then reduces to the simple form

$$b = c - \frac{R}{2\tau} [F(\sigma_A, \sigma_T, \Delta T) - F(\sigma_A^s, \sigma_T, \Delta T)]. \quad (85)$$

It should be noted that the stress transfer function $C(z)$, defined by (68)-(70), together with its first two derivatives are continuous everywhere in the region $0 \leq z \leq L$, automatically ensuring the continuity of the shear stress σ_{rz} , the radial stress σ_{rr} , the axial stress σ_{zz} , the radial displacement u_r and the average axial displacement \bar{u}_z , in both the fibre and matrix. The axial displacement component u_z is discontinuous on $z = b$ and $z = c$ in both the fibre and matrix except at the interface. This is only continuity requirement that cannot be satisfied by the constant interfacial shear stress model. The achievement of the required continuity for all other stress and displacement components, including the average axial displacement \bar{u}_z , indicates that the constant interfacial shear stress model developed in this paper is a significant improvement over other models that have often been based on shear-lag theory (see Section 13 for further discussion).

11 Solution for a sliding interface with Coulomb friction

In the presence of a fibre fracture or matrix crack, the assumption of a constant interfacial shear stress is frequently made in the literature, although the Coulomb

friction law is more acceptable from a physical point of view as the interfacial shear stress is expected to depend on the compressive normal stress at the interface. At relatively low applied loads, a frictionally bonded interface between fibre and matrix is expected to behave as a perfectly bonded interface, as described in Section 9. As the maximum interfacial shear stress was predicted in Section 9 to occur away from the crack plane, initial frictional slipping is likely to be a local event where the slip zone is wholly embedded in the interface and it gradually increases in length as load is applied. Such growth would be expected to occur at both ends of the slip zone until one of the slip zone boundaries reaches the crack plane. At first sight, the analysis of the early stages of frictional slip would appear to be very complex. However, it has to be remembered that the stress analysis is approximate and that a more accurate solution would exhibit a shear stress singularity at the location of the interface with the crack plane, implying that frictional slip would initiate at this singularity. It is, therefore, reasonable to assume that the frictional slip zone initiates at the crack plane and progressively grows along the fibre/matrix interface. The analysis will assume that the fibre and matrix are always in mechanical contact at all points along the sliding interface, and it may not, therefore, be applicable for all states of loading. Solutions obtained will be valid only if they have been checked to ensure that the interface exhibits compression or zero loading along the entire sliding zone.

Consider now the geometry of the fibre, matrix and sliding interface shown in Fig. 3. The fibre has radius R and there is a fibre fracture or matrix crack at the location $z = L$. The representation for the stress and displacement fields defined in Section 4 apply to both stress transfer regions shown in Fig. 3.

The Coulomb friction law is specified, for all z lying in the interfacial slip zone, by

$$\lambda \sigma_{rz}(R, z) = \eta \sigma_{rr}(R, z), \quad (86)$$

where $\eta > 0$ is the coefficient of friction and where solutions are valid only if $\sigma_{rr} \leq 0$ in the sliding zone so that there is mechanical contact between the fibre and matrix in this zone. The sign of the interfacial shear stress $\sigma_{rz}(R, z)$ will depend on the type of problem being solved; negative for matrix cracks and positive for fibre fractures. In (86) the value of the parameter $\lambda = -1$ for fibre fractures and $\lambda = 1$ for matrix cracks. From (14), (15) and (30)

$$\begin{aligned} \sigma_{rz}^f(R, z) &= \frac{1}{2}RC'(z), \\ \sigma_{rr}^f(R, z) &= fR^2C''(z) - hC(z) - \rho, \end{aligned} \quad (87)$$

where

$$f = \frac{\alpha - \gamma V_m}{V_f} - \frac{3 + \nu_T^f}{16}, h = \beta \frac{V_m}{V_f}, \rho = V_m \frac{\phi}{R^2} - \sigma_T, \quad (88)$$

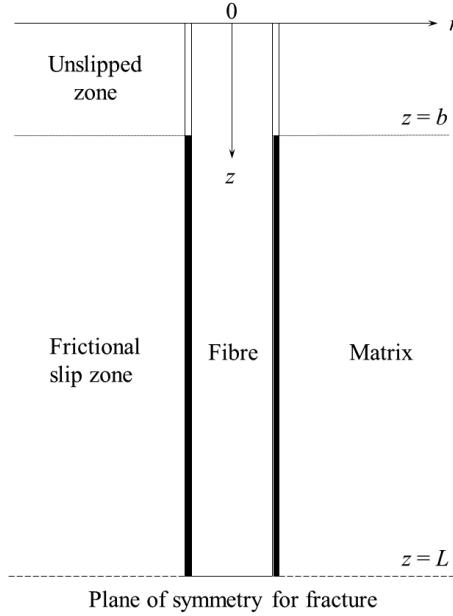


Figure 3: Schematic diagram showing the geometry for a sliding interface associated with a fibre fracture or matrix crack when Coulomb friction is assumed.

and where α , β , γ and ϕ are defined by (28), (31) and (A12). On substituting (87) into (86) it can be shown that in the slip zone the stress transfer function $C(z)$ must satisfy the following second order ordinary differential equation

$$fR^2C''(z) - 2\lambda gRC'(z) - hC(z) = \rho, \text{ where } g = \frac{1}{4\eta}. \quad (89)$$

It should be noted that the effective axial stress σ_A and the axial strain ϵ_A for an undamaged composite are related according to the effective stress-strain relation (A23). The differential equation (89) applies only in the sliding region $b \leq z \leq L$ where frictional slip occurs governed by the Coulomb law (86).

The stress transfer function that is used for the sliding region where frictional slip is governed by the Coulomb law must satisfy the ordinary differential equation (89), and the boundary conditions $C'(\pm L) = 0$ and (52) on $z = L$. The required solution of the differential equations (41) and (89) is given by

For $0 \leq z \leq b$

$$C(z) = A^* \cosh \frac{(p+q)z}{R} + B^* \cosh \frac{(p-q)z}{R}, \quad (90)$$

For $b \leq z \leq L$

$$C(z) = \Omega \left[v \exp \left(-u \frac{L-z}{R} \right) - u \exp \left(-v \frac{L-z}{R} \right) \right] - \frac{\rho}{h}, \quad (91)$$

where ρ is defined by (88) and

$$\Omega = \frac{\frac{\rho}{h} + F(\sigma_A, \sigma_T, \Delta T)}{v - u}, u = \frac{\lambda g}{f} + \sqrt{\frac{g^2}{f^2} + \frac{h}{f}}, v = \frac{\lambda g}{f} - \sqrt{\frac{g^2}{f^2} + \frac{h}{f}}. \quad (92)$$

For applications to be considered here, it is found that $h/f > 0$ so that $u > 0$ and $v < 0$ for all values of $g = 1/(2\eta) \geq 0$. From (91)

$$C'(z) = \Omega uv \left[\exp \left(-u \frac{L-z}{R} \right) - \exp \left(-v \frac{L-z}{R} \right) \right], \quad (93)$$

and since $u - v < 0$, it is clear that $C'(z)$ does not change sign in the region $b \leq z \leq L$. The boundary conditions $C'(L) = 0$ and (52) are sufficient to determine the function $C(z)$ uniquely for the sliding region $b \leq z \leq L$ as seen from the result (91). In (90) the parameters A^* and B^* are selected so that the function $C(z)$ and its first derivative are both continuous at the point $z = b$. On letting $\zeta = (L - b)/R$, it can be shown that

$$\begin{aligned} A^* &= \Lambda^* \frac{C_1(\zeta) - (p-q) \tanh \frac{(p-q)b}{R} C_0(\zeta)}{\cosh \frac{(p+q)b}{R}}, \\ B^* &= \Lambda^* \frac{(p+q) \tanh \frac{(p+q)b}{R} C_0(\zeta) - C_1(\zeta)}{\cosh \frac{(p-q)b}{R}}, \end{aligned} \quad (94)$$

where

$$\frac{1}{\Lambda^*} = (p+q) \tanh \frac{(p+q)b}{R} - (p-q) \tanh \frac{(p-q)b}{R}, \quad (95)$$

and where

$$\begin{aligned} C_0(\zeta) &= C(b) = \Omega[v \exp(-u\zeta) - u \exp(-v\zeta)] - \frac{\rho}{h}, \\ C_1(\zeta) &= RC'(b) = \Omega uv[\exp(-u\zeta) - \exp(-v\zeta)]. \end{aligned} \quad (96)$$

A criterion for the location of the boundary $z = b$ between the unslipping and sliding zones has not yet been given. The appropriate criterion is to expect that the Coulomb friction law (89) is satisfied by the stress field in the unslipped zone at the point $z = b$. It is clear from the continuity of $C(z)$ and $C'(z)$ at $z = b$, and (14), (15) and (30), that such a condition is automatically satisfied if the function $C''(z)$ is also continuous at $z = b$, a situation that arises if the following transcendental equation determining the value of $\zeta = (L - b)/R$ is satisfied

$$\begin{aligned} (p^2 - q^2) &\left((p - q) \tanh \frac{(p + q)(L - R\zeta)}{R} - (p + q) \tanh \frac{(p - q)(L - R\zeta)}{R} \right) C_0(\zeta) \\ &+ 4pqC_1(\zeta) - \left((p + q) \tanh \frac{(p + q)(L - R\zeta)}{R} - (p - q) \tanh \frac{(p - q)(L - R\zeta)}{R} \right) C_2(\zeta) = 0, \end{aligned} \quad (97)$$

where

$$C_2(\zeta) = R^2 C''(b) = \Omega uv[u \exp(-u\zeta) - v \exp(-v\zeta)]. \quad (98)$$

It should be noted that for the case of frictional slip in the sliding zone governed by the Coulomb law, the stress transfer function $C(z)$ defined by (90) and (91), together with the first two derivatives, are continuous everywhere in the region $0 \leq z \leq L$, automatically ensuring the continuity of the shear stress σ_{rz} , the radial stress σ_{rr} , the axial stress σ_{zz} , and the radial displacement u_r .

The axial displacement component u_z is discontinuous on $z = b$ in both the fibre and the matrix except at the interface. This is the only continuity requirement that cannot be satisfied by the Coulomb friction model. The achievement of the required continuity for all other stress and displacement components, including the average axial displacement \bar{u}_z , indicates that the Coulomb friction model developed in this paper is one of high quality with regard to the satisfaction of boundary and interface conditions.

While the condition (97) is used to determine a value for $\zeta = (L - b)/R$ and thus the location $z = b$ of the boundary between the slip zone and the unslipped region, it can be used also to determine the condition that is placed on the parameters σ_A , σ_T and ΔT such that $b = L$, i.e. such that the length of the slip zone is zero. It is

easily shown using (96)-(98) that $b = L$ so that $\zeta = 0$ whenever

$$G(\sigma_A, \sigma_T, \Delta T) \equiv (p+q) \left[\{(p-q)^2 + uv\} F(\sigma_A, \sigma_T, \Delta T) + uv \frac{\rho}{h} \right] \tanh \frac{(p+q)L}{R} \\ - (p-q) \left[\{(p+q)^2 + uv\} F(\sigma_A, \sigma_T, \Delta T) + uv \frac{\rho}{h} \right] \tanh \frac{(p-q)L}{R} = 0. \quad (99)$$

It follows from (88), (52), (A16), (A17), (A28) and (A29) that the function G defined by (99) is linear in the quantities σ_A , σ_T and ΔT so that

$$G(\sigma_A, \sigma_T, \Delta T) \equiv G_1 \sigma_A + G_2 \sigma_T + G_3 \Delta T = 0, \quad (100)$$

where the coefficients are most easily found numerically using the relations

$$G_1 = G(1, 0, 0), G_2 = G(0, 1, 0), G_3 = G(0, 0, 1). \quad (101)$$

Clearly the axial stress for which $b = L$ is given by

$$\sigma_A = -\frac{G_2 \sigma_T + G_3 \Delta T}{G_1}. \quad (102)$$

It should be noted that the axial stress determined by (102) does not depend on the value of λ as it follows from (92) that $uv = -h/f$.

In Appendix B is given an analysis that determines the condition (B17) for which contact at the interface is lost between fibre and matrix; a situation for which the radial and shear stresses at the interface in the sliding zone are zero everywhere. The relations (99) or (100) and (B17) may be used to determine the applied axial stress range for which solutions with sliding governed by the Coulomb friction law may be found.

12 An illustrative example

Three types of model associated with fibre fractures or matrix cracks have been developed in this paper. In Section 9 the interface was assumed not to slide for all states of loading. In Section 10 an interface sliding model was developed that assumed that the sliding interface is characterised by a uniform interfacial shear stress τ , although a transition zone had to be introduced in order to satisfy all traction boundary conditions on the crack surfaces. In Section 11 a model was developed where interfacial sliding was characterised by the Coulomb friction law. In all cases it was assumed that the undamaged composite was frictionally bonded meaning that bonding between fibre and matrix is so small that it can be neglected. It is beyond the scope of this paper to consider the application of the models to the

range of materials to which they are relevant. The approach taken here is to select just one material and to investigate thoroughly the important characteristics of each type of stress transfer model.

As the case of carbon fibre composites highlights a problem, to be discussed below, it is chosen as the material to be considered is an example. The radius of the fibres is $3.5 \mu m$, the volume fraction of fibres will be taken as 0.5 or 0.6, and the temperature and stress-free temperature are such that $\Delta T = -85^\circ C$ or $\Delta T = 85^\circ C$. The properties assumed for the carbon fibre and the epoxy matrix are given by:

	Fibre	Matrix
E_A (GPa)	208.0	3.89
E_T (GPa)	16.7	3.89
μ_A (GPa)	18.0	1.41971
ν_A	0.25	0.37
ν_T	0.35	0.37
α_A ($/^{\circ}C \times 10^6$)	1.1	55.0
α_T ($/^{\circ}C \times 10^6$)	22.1	55.0

For these properties the volume fraction of 0.5 leads to a real value of the parameter q defined by (54) and a volume fraction of 0.6 leads to a pure imaginary value.

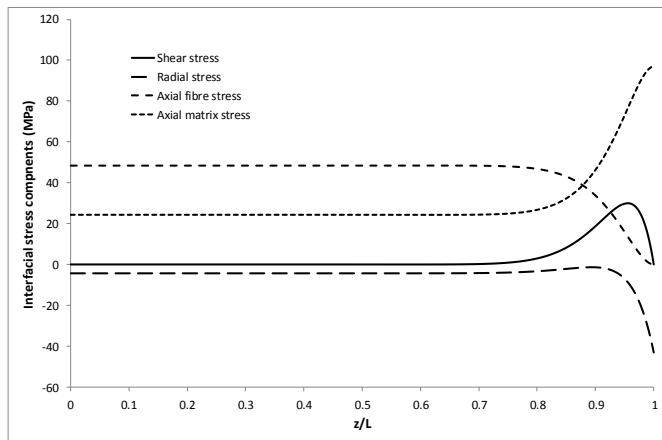


Figure 4: Interfacial stress distributions for an unslipped interface in a CFRP composite having fibre fractures that lead to a shear stress having a maximum magnitude of 30 MPa. ($V_f = 0.6$, $\sigma_A = 0.0388$ GPa, $\Delta T = -85^\circ C$, fibre crack density = $20/mm$)

Consider a representative volume element (concentric cylinders comprising a single

fibre plus surrounding matrix) of a composite before interfacial slippage, having fibre volume fraction 0.6 (so that q is an imaginary quantity), in which the fibre has fragmented into equal lengths $2L$ of $50\mu\text{m}$, i.e. a fibre crack density of $20/\text{mm}$. A uniaxial axial stress of 0.03876909 GPa is applied so that the maximum interfacial stress is 30 MPa exactly. Fig. 4 shows the axial stress distributions in both the fibre and matrix as a function of z/L , together with the interfacial shear and normal stresses.

It should be noted that the stresses are all continuous, that the interfacial shear stress has an imposed maximum value of 30 MPa at the location $z = c$ where $c/L = 0.9553$, and that the normal stress is everywhere compressive. The axial fibre stress is seen to diminish to a zero value at the location $z = L$ of the fibre fracture. The axial matrix stress increases to its maximum value on the plane of fibre fracture.

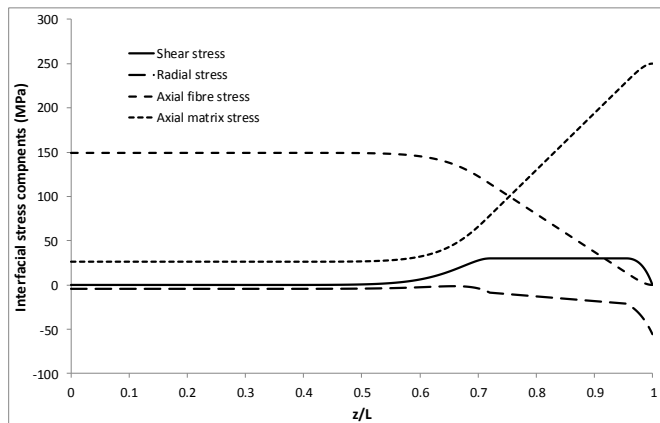


Figure 5: Interfacial stress distributions for a sliding interface in a CFRP composite having fibre fractures that lead to a uniform shear stress having a maximum magnitude of 30 MPa . ($V_f = 0.6$, $\sigma_A = 0.1\text{ GPa}$, $\Delta T = -85^\circ\text{C}$, fibre crack density = $20/\text{mm}$)

It is now assumed that the stress distributions shown in Fig. 4 characterise the stress state for the initiation of fibre/matrix sliding where the magnitude of the interfacial shear stress in the sliding zone is assumed to have a uniform value of 30 MPa . The same fibre crack density of $20/\text{mm}$ is used. When the applied stress is increased to a value of 0.1 GPa the resulting stress distributions are shown in Fig. 5. The corresponding displacement distributions are shown in Fig. 6 where the displacements shown are normalised with respect to the fibre radius R . It should be noted that for this case the approximate formulae (65) and (85) determining the values of

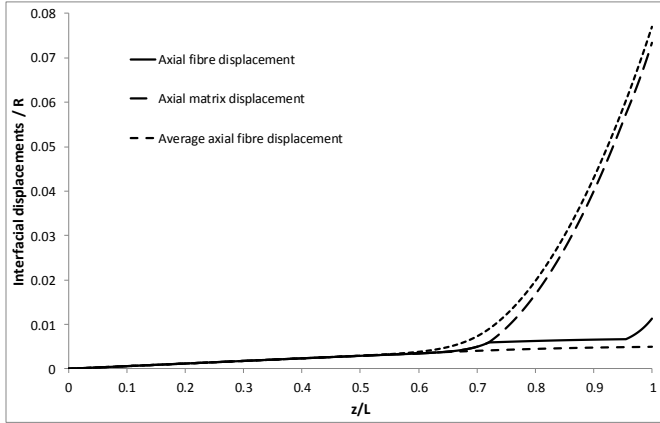


Figure 6: Interfacial displacement distributions for a sliding interface in a CFRP composite having fibre fractures that lead to a shear stress having a maximum magnitude of 30 MPa. ($V_f = 0.6$, $\sigma_A = 0.1\text{GPa}$, $\Delta T = -85^\circ\text{C}$, fibre crack density = $20/\text{mm}$)

the parameters b and c , which define the boundaries of the constant shear stress region, are extremely accurate implying negligible interaction of neighbouring fibre fractures.

The major characteristics of the solution are as follows:

Stress distributions

- The interfacial shear stress has the uniform value 30 MPa in the region $0.7202 \leq z \leq 0.9533$.
- The interfacial shear stress and fibre stress tend to zero as the fibre fracture at $z = L$ is approached. In the transition zone $0.9533 \leq z/L \leq 1$, the stress distribution enables the attainment of a zero shear stress in the matrix at $z = L$.
- The interfacial radial stress is everywhere compressive.
- The interfacial shear and axial stresses are smooth, but the radial stress has sharp corners at the points $z = b$ and $z = c$.

Displacement distributions

- The distributions of interfacial axial displacement for fibre and matrix are identical in the unslipped region $0 \leq z/L \leq 0.7202$ of the interface.

- The interfacial and average values of the axial displacements of the fibre and matrix are very similar and continuous.

When the fibre is intact, but the matrix has cracked instead, it is much more difficult to obtain solutions as the magnitude of the maximum interfacial shear stress for an unslipped interface is much lower than for the fibre fracture case. If the fibre fracture case just described is applied instead to a matrix crack no solutions can be found as the imposed critical interfacial shear stress τ of 30 MPa is very much larger than the magnitude of the maximum shear stress (10.853 MPa) that will occur for an unslipped interface. To provide an example prediction for a matrix crack, the volume fraction is now reduced to 0.5 (so that q is a real quantity) and the value of τ is taken as 10 MPa. The resulting stress distributions are shown in Fig. 7 for the CFRP composite having the fibre and matrix properties assumed above. The axial fibre stress distribution is not shown as the vertical axis would need to be extended to 200 MPa. For this case, the approximate formulae (65) and (85), defining values for b and c , are again very accurate implying negligible interaction of neighbouring matrix cracks.

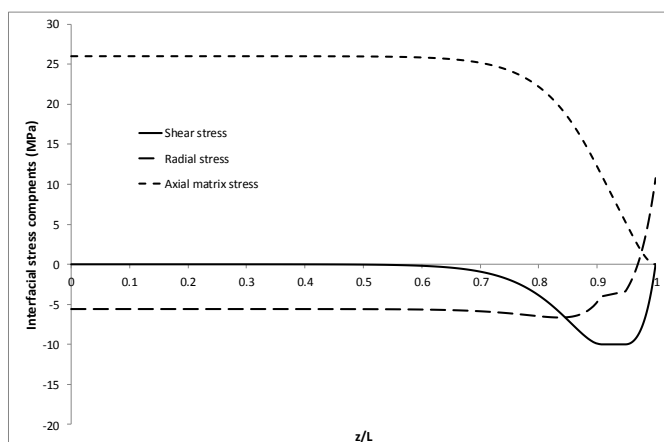


Figure 7: Interfacial stress distributions for a sliding interface in a CFRP composite having matrix cracks that lead to a shear stress having a maximum magnitude of 10 MPa. ($V_f = 0.5$, $\sigma_A = 0.1\text{GPa}$, $\Delta T = -85^\circ\text{C}$, fibre crack density = $20/\text{mm}$)

It is clear that the radial stress is not compressive in the whole of the transition zone thus violating an important modelling requirement. An example has thus been identified indicating that the constant interfacial shear stress model for sliding is inadequate. If, however, the interfacial shear stress τ is now set to the much lower

value of 2 MPa the interfacial radial stress is then always negative, thus providing a more acceptable solution. The sliding region is extensive for this case and some crack interaction occurs. To remove this interaction the matrix crack density is reduced to the value $10/mm$ and the resulting stress distributions are shown in Fig. 8.

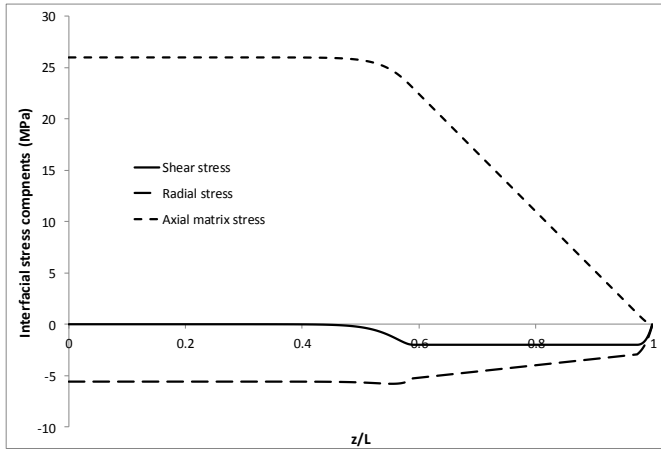


Figure 8: Interfacial stress distributions for a sliding interface in a CFRP composite having matrix cracks that lead to a shear stress having a maximum magnitude of 2 MPa. ($V_f = 0.5$, $\sigma = 0.1GPa$, $\Delta T = -85^\circ C$, fibre crack density = $10/mm$)

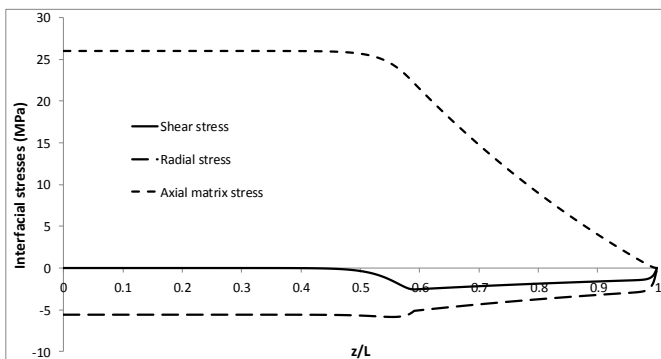


Figure 9: Interfacial stress distributions for a sliding interface in a CFRP composite having matrix cracks subject to Coulomb friction. ($V_f = 0.5$, $\sigma_A = 0.1GPa$, $\Delta T = -85^\circ C$, fibre crack density = $10/mm$, $\eta = 0.5$)

It is seen that the interfacial radial stress is always negative as required.

This completes the discussion of the model of interface sliding based on the popular concept of imposing a uniform interfacial shear stress, but combined in this paper with a transition zone to prevent the violation of the zero shear stress boundary condition on the crack surfaces. The second type of sliding model described in Section 11 makes use of the Coulomb friction law. The previous problem that generated the results in Fig. 8 is now solved using the Coulomb friction model. The coefficient of friction η is selected to be 0.5 and the resulting stress and displacement distributions are shown in Figs. 9 and 10.

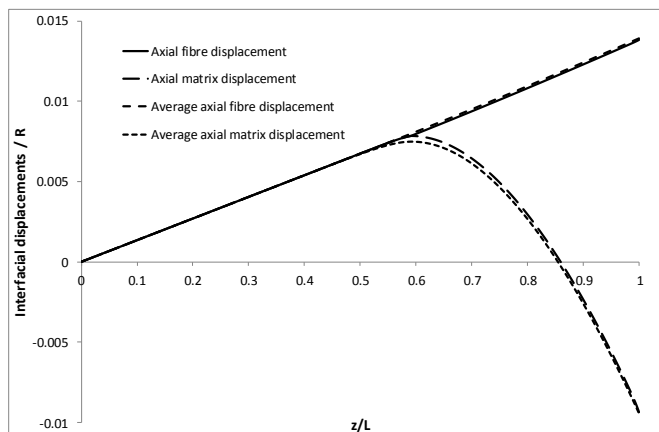


Figure 10: Interfacial displacement distributions for a sliding interface in a CFRP composite having matrix cracks subject to Coulomb friction. ($V_f = 0.5$, $\sigma_A = 0.1\text{GPa}$, $\Delta T = -85^\circ\text{C}$, fibre crack density = $10/\text{mm}$, $\eta = 0.5$)

Again, the axial fibre stress distribution is not shown as the vertical axis would need to be extended to 200 MPa. The major characteristics of the solution are as follows:

Stress distributions

- The interfacial shear stress is non-uniform in the sliding region $0.5909 \leq z/L \leq 1$.
- The interfacial shear stress and fibre stress tend to zero as the fibre fracture at $z = L$ is approached. No transition zone is included in the model although the stress distribution does indicate an apparent transition zone near $z = L$ that is similar to that used in the constant shear model (see Fig. 8). This apparent transition is predicted automatically when solving the differential equation (89).

- The interfacial radial stress is everywhere compressive.
- The interfacial shear and axial stresses are smooth but the radial stress has a sharp corner at the point $z = b$.
- Acceptable solutions, where there is interfacial contact along the whole length of the sliding zone, are possible only if the applied axial stress lies in the range $0.424 \leq \sigma_A \leq 1.163$ (GPa).

Displacement distributions

- The distributions of interfacial axial displacement for fibre and matrix are identical in the unslipped region $0 \leq z/L \leq 0.5909$ of the interface.
- The interfacial and average values of the axial displacements of the fibre and matrix are almost coincident, and they are continuous.

It should be noted that the results for the interfacial shear and normal stresses shown in Figs. 8 and 9 are very similar when using a relatively large value 0.5 for the coefficient of friction. This similarity indicates that for friction problems, the values of τ used in the constant shear stress model need to be relatively small. However, it is worth mentioning that fibre fracture problems can be solved using much larger values of τ , and such values can be justified if the model is being used to predict (approximately) shear yielding phenomena associated with matrix plasticity that can occur in the matrix near fibre fractures.

When solving problems, it is useful to determine the applied stress for which the fibre and matrix are expected to separate along the sliding interface. The analysis given in Appendix B considers this aspect of interface sliding problems. For the example being considered where $\sigma_T = 0$ and $\Delta T = -85^\circ\text{C}$, the value of the axial stress at which separation occurs is $\sigma_A = 1.163$ GPa (not a value of practical relevance), and if this value is used in the Coulomb friction model the interfacial shear and normal stresses are zero everywhere along the interface. At this critical applied stress, the interface has slipped entirely because of the assumption of frictional bonding.

If the example is now applied to a fibre fracture rather than a matrix crack, keeping all the other parameters fixed, then it is not easy to obtain solutions. It is not in fact possible to find appropriate solutions of the equation (83) unless the applied stress σ_A lies in the range $-14.7(\text{MPa}) \leq \sigma_A \leq 7.762(\text{MPa})$, values which are very small from a practical viewpoint. This identifies the problem alluded to above with regard to the use of carbon fibres in an epoxy matrix as an example material. At the critical value $7.762(\text{MPa})$, the length of the slipping zone is zero and the solution

for an unslipped interface is obtained. Solutions obtained at other applied stresses in this range lead to tensile interfacial normal stresses in the sliding zone which are not acceptable. One way of achieving negative normal stresses is to use a positive value of the temperature difference ΔT . When the fibre fracture example is solved with the value $\Delta T = 85^\circ\text{C}$ at an applied stress of 12 MPa, the results shown in Figs. 11 and 12 are obtained.

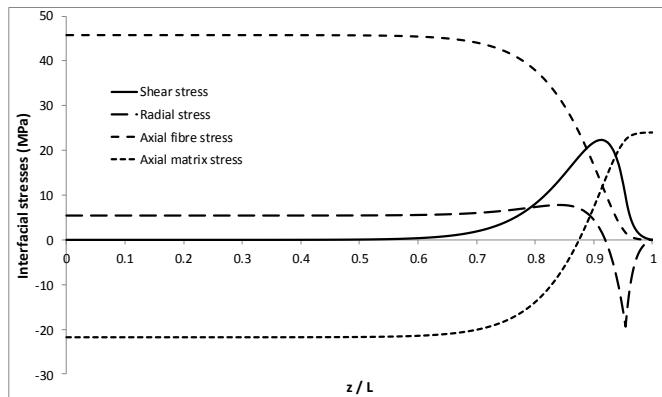


Figure 11: Interfacial stress distributions for a sliding interface in a CFRP composite having fibre cracks subject to Coulomb friction. ($V_f = 0.5$, $\sigma_A = 12\text{MPa}$, $\Delta T = 85^\circ\text{C}$, fibre crack density = $10/\text{mm}$, $\eta = 0.5$)

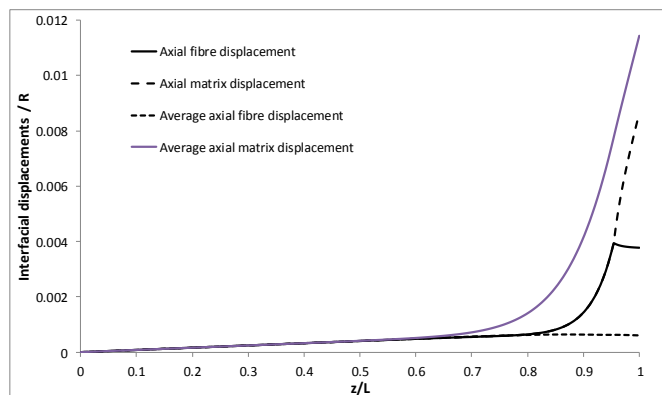


Figure 12: Interfacial displacement distributions for a sliding interface in a CFRP composite having fibre fractures subject to Coulomb friction. ($V_f = 0.5$, $\sigma_A = 12\text{MPa}$, $\Delta T = 85^\circ\text{C}$, fibre crack density = $10/\text{mm}$, $\eta = 0.5$)

The sliding zone occupies the region $0.9543 \leq z/L \leq 1$, and it is seen that the interfacial radial stress is negative in the sliding zone as required for valid solutions. Contact is lost in the sliding zone when the applied stress σ_A exceeds the value 14.7 MPa. Clearly interfacial sliding for a frictionally bonded composite is a very limited occurrence when considering fibre fractures. In fact, acceptable solutions for this case, where there is interfacial contact along the whole length of the sliding zone, are possible only if the applied axial stress lies in the very limited range $-7.762(\text{MPa}) \leq \sigma_A \leq 14.7(\text{MPa})$. It should be noted that changing the sign of ΔT does not alter the magnitudes of the bounds found for σ_A . They are merely reversed because the example has assumed that the transverse applied stress $\sigma_T = 0$.

The results obtained using the Coulomb friction law for fibre fractures suggest that a more complex type of frictional contact must occur when the applied axial stress lies outside this range involving both a frictional slip region and an open region where contact has been lost. An investigation of this type of stress transfer is beyond the scope of this paper.

13 Discussion

The analysis and results presented in this paper apply only to frictionally bonded composites, i.e. to composites where interfacial bonding is very weak so that the interfacial fracture energy for fibre/matrix debonding can be neglected. In practice, composite manufacturers attempt to achieve high levels of interface bonding, especially for polymer composites. It is remarked that for ceramic matrix composites weak interfaces are desirable so that damage will form as multiple cracking rather than as the propagation of a single dominant crack.

A key characteristic of the stress transfer model that has been described in detail in this paper concerns the achievement of the satisfaction of the required field equations, boundary and interface conditions. Many of the required equations and conditions are satisfied exactly, while the axial stress-strain relations for fibre and matrix are satisfied on averaging over fibre or matrix. Such averages are a reasonable approximation for composites for which the volume fraction is not too small (as in fragmentation tests) or too large. Shear-lag approaches that provide some comparable analytical results, are based on various approximations that are causes for concern from a mechanics point of view. It is useful now to identify clearly these approximations. The first approximation that is made concerns the neglect, for both the fibre and matrix, of the terms $\partial u_r / \partial z$ in the expressions for the shear strain ϵ_{rz} . This assumption is expected to lead to significant errors. The second approximation that is usually made is the assumption that the axial Poisson's ratios in fibre and matrix is zero. This assumption is also expected to lead to significant errors. It is observed that shear-lag models do not consider some of the equilib-

rium equations and some of the stress-strain relations, indicating further sources of significant error. It is concluded, that while shear-lag approaches are relatively easy to develop and understand, they do suffer from having to make a number of assumptions that are expected to lead to unacceptable errors.

While the models developed in this paper do not suffer from the deficiencies just described in connection with the use of shear-lag approaches, it must be emphasised that this does not necessarily mean that the models will generate accurate results. For example, the models derived assume that the axial stresses in both the fibre and matrix have values that differ but are independent of the radial coordinate. This will not be a characteristic of the exact solution, especially in the plane of the fibre or matrix cracks where singularities are known to exist at the fibre/matrix interface. For perfectly bonded composites, exact solutions to the stress transfer problems would predict that the shear stress and axial stress would be singular at the interface in the uncracked fibre if the matrix is cracked or in the uncracked matrix if the fibre is broken. Such predictions are beyond the capabilities of the concentric cylinder model described in this paper. However, unpublished work has been undertaken by the author that applies the stress and displacement representation derived in Sections 4-7 to an assembly of multiple concentric cylinders enabling the stress singularities at debond tips to be well represented. This is achieved by sub-dividing the fibre and matrix into systems of concentric cylindrical layers in which the axial stress is uniform but which differ from layer to layer. To date solutions have been derived only for perfectly bonded interfaces. Much further work is needed to extend the multiple cylinder model to include sliding and debonded zones.

Beyond the scope of this paper is the consideration of composites having strong fibre/matrix bonding. It is, however, useful to note that much of the analysis presented applies also to this important type of composite. One approach is to regard the debond length $L - b$ as a given parameter in which case it is required to determine the stress and displacement distributions in the fibre and matrix that correspond to this debond length. This is achieved simply by removing from the analysis the requirement that either the condition (83) or (97) is satisfied. This means that the second derivative of the stress transfer function $C(z)$ is not continuous at the location $z = b$ of the debond tip. As a consequence, the interfacial normal stress will be discontinuous at this point where exact solutions are expected to predict a singularity, as mentioned above.

14 Conclusion

An analytical model of stress transfer has been described that can be used to predict the localised stress and displacement distributions associated with fibre fractures and matrix cracks in unidirectional composites whose fibres and matrix deform

linear elastically and are subject to differing thermal expansion properties. The approach to modelling interfacial sliding has been to ensure that, wherever possible, the expressions for all relevant physical parameters are given by analytical formulae. The stress transfer associated with sliding can be modelled using two different approaches. The first assumes that the interfacial shear stress is uniform in the sliding zone. Satisfactory solutions, enabling zero shear tractions on crack surfaces, are possible only if a transition zone is included in the neighbourhood of the fibre fracture or matrix crack. The second approach assumes that stress transfer in the sliding region is governed by the Coulomb friction law; a situation that does not require the use of a transition zone. Predictions to date (not all included in this paper) indicate that the stress transfer models work very well for a range of composite types and loading conditions that lead to compressive interfacial normal stresses along the entire length of the sliding zone.

Acknowledgement: The author would like to acknowledge the Materials Programme of the National Measurement Office, Department of Innovation, Universities and Skills, UK.

References

- Aveston, J.; Cooper, G. A.; Kelly, A.** (1971): *Single and multiple fracture*, in *Conference on the Properties of Fibre Composites*. IPC Science and Technology Press, Guildford, Surrey, UK.
- Hutchinson, J. W.; Jensen, H. M.** (1990): Models of fiber debonding and pull-out in brittle composites with friction. *Mech. Mater.*, vol. 9, pp. 139–163.
- McCartney, L. N.** (1987): Mechanics of matrix cracking in brittle matrix fibre reinforced composites. *Proc. Roy. Soc. Lond.*, vol. A409, pp. 329.
- McCartney, L. N.** (1989): New theoretical model of stress transfer between fibre and matrix in a uniaxially fibre reinforced composite. *Proc. Roy. Soc. London.*, vol. A425, pp. 215–244.
- McCartney, L. N.** (1991): Analytical models of stress transfer in unidirectional composites and cross-ply laminates, and their application to the prediction of matrix/transverse cracking. In *Proc. IUTAM Symposium on 'Local mechanics concepts for composite materials systems'*, pp. 251–282, Blacksburg, Va.
- McCartney, L. N.** (1992): Mechanics for the growth of bridged cracks in composite materials: Part I, basic principles. *J. Comp. Tech. & Res.*, vol. 14, pp. 133–146.

McCartney, L. N. (1992): Mechanics for the growth of bridged cracks in composite materials: Part II, applications. *J. Comp. Tech. & Res.*, vol. 14, pp. 147–154.

McCartney, L. N. (1996): Stress transfer mechanics: Models that should be the basis of life prediction methodology. In W.S. Johnson, J. L.; Cox, B.(Eds): *Life prediction methodology for titanium matrix composites*, ASTM STP 1253, pp. 85–113.

McCartney, L. N. (1999): Analytical model for debonded interfaces associated with fibre fractures and matrix cracks. In *Proc. ICCM 12*, Paris.

Nairn, J. A. (1992): A variational mechanics analysis of the stresses around breaks in embedded fibres. *Mech. Mater.*, vol. 13, pp. 131–154.

Nairn, J. A. (1997): On the use of shear-lag methods for analysis of stress transfer in unidirectional composites. *Mech. Mater.*, vol. 26, pp. 63–80.

Reissner, E. (1950): On a variational theorem in elasticity. *J. of Math. Phys.*, vol. 29, pp. 90–95.

Appendix A: Elasticity analysis of two concentric cylinders

The following analysis applies to two concentric perfectly bonded cylinders having external radii R and $a > R$, subject to a uniform temperature change ΔT , that is subject to a uniform axial strain ϵ_A and uniform transverse stress σ_T on the external surface of the outer cylinder. A set of cylindrical polar coordinates (r, θ, z) will be used where the origin lies on the axis of the inner cylinder.

The fibre and matrix are regarded as a transverse isotropic solids so that their stress-strain-temperature relations are of the form (3)-(6), and the stress field must satisfy the equilibrium equations (1) and (2). The boundary and interface conditions that must be satisfied are

$$\sigma_{rr}^m(a, z) = \sigma_T, \quad (\text{A1})$$

$$\sigma_{rz}^m(a, z) = 0, \quad (\text{A2})$$

$$\sigma_{rr}^m(R, z) = \sigma_{rr}^f(R, z), \quad (\text{A3})$$

$$\sigma_{rz}^m(R, z) = \sigma_{rz}^f(R, z), \quad (\text{A4})$$

$$u_r^m(R, z) = u_r^f(R, z), \quad (\text{A5})$$

$$u_z^m(R, z) = u_z^f(R, z), \quad (\text{A6})$$

Solutions are considered such that

$$u_z^f \equiv u_z^m \equiv \epsilon_A z. \quad (\text{A7})$$

The solution for an undamaged composite is of the following classical Lamé form

$$u_r^f = A_f r, u_\theta^f \equiv 0, \quad (\text{A8})$$

$$u_r^m = A_m r + \frac{\phi}{2\mu_T^m r}, u_\theta^m \equiv 0, \quad (\text{A9})$$

where A_f , A_m and ϕ are constants defined by

$$A_f = -v_A^f \varepsilon_A + (\alpha_T^f + v_A^f \alpha_A^f) \Delta T + \frac{1}{2k_T^f} \left(\sigma_T - V_m \frac{\phi}{R^2} \right), \quad (\text{A10})$$

$$A_m = -v_A^m \varepsilon_A + (\alpha_T^m + v_A^m \alpha_A^f) \Delta T + \frac{1}{2k_T^m} \left(\sigma_T + V_f \frac{\phi}{R^2} \right), \quad (\text{A11})$$

$$\frac{\phi}{R^2} = \lambda \left[(v_A^m - v_A^f) \varepsilon_A + (\alpha_T^f + v_A^f \alpha_A^f) \Delta T - (\alpha_T^m + v_A^m \alpha_A^m) \Delta T + \frac{1}{2} \left(\frac{1}{k_T^f} - \frac{1}{k_T^m} \right) \sigma_T \right], \quad (\text{A12})$$

where

$$\frac{1}{\lambda} = \frac{1}{2} \left(\frac{1}{\mu_T^m} + \frac{V_f}{k_T^m} + \frac{V_m}{k_T^f} \right), \frac{1}{k_T^f} = \frac{2(1 - \nu_T^f)}{E_T^f} - \frac{4(\nu_A^f)^2}{E_A^f}, \frac{1}{k_T^m} = \frac{2(1 - \nu_T^m)}{E_T^m} - \frac{4(\nu_A^m)^2}{E_A^m}. \quad (\text{A13})$$

On differentiating the displacement field it follows that the non-zero strain components are

$$\varepsilon_{rr}^f = \frac{\partial u_r^f}{\partial r} = A_f, \varepsilon_{\theta\theta}^f = \frac{u_r^f}{r} = A_f, \varepsilon_{zz}^f = \varepsilon_A, \quad (\text{A14})$$

$$\varepsilon_{rr}^m = \frac{\partial u_r^m}{\partial r} = A_m - \frac{\phi}{2\mu_T^m r^2}, \varepsilon_{\theta\theta}^m = \frac{u_r^m}{r} = A_m + \frac{\phi}{2\mu_T^m r^2}, \varepsilon_{zz}^m = \varepsilon_A. \quad (\text{A15})$$

The corresponding non-zero stress components are

$$\sigma_{rr}^f = \sigma_T + \phi \left(\frac{1}{a^2} - \frac{1}{R^2} \right) = \sigma_T - V_m \frac{\phi}{R^2}, \quad (\text{A16})$$

$$\sigma_{\theta\theta}^f = \sigma_T + \phi \left(\frac{1}{a^2} + \frac{1}{R^2} \right) = \sigma_T + V_m \frac{\phi}{R^2}, \quad (\text{A17})$$

$$\sigma_{zz}^f = \sigma_f = E_A^f (\epsilon_A - \alpha_A^f \Delta T) + 2\nu_A^f (\sigma_T - V_m \frac{\phi}{R^2}), \quad (\text{A18})$$

$$\sigma_{rr}^m = \sigma_T + \phi \left(\frac{1}{a^2} - \frac{1}{r^2} \right), \quad (\text{A19})$$

$$\sigma_{\theta\theta}^m = \sigma_T + \phi \left(\frac{1}{a^2} + \frac{1}{r^2} \right), \quad (\text{A20})$$

$$\sigma_{zz}^m = \sigma_m = E_A^m (\epsilon_A - \alpha_A^m \Delta T) + 2\nu_A^m \left(\sigma_T + V_f \frac{\phi}{R^2} \right). \quad (\text{A21})$$

The effective axial stress σ_A is defined by the relation

$$\sigma_A = V_f \sigma_f + V_m \sigma_m, \quad (\text{A22})$$

and it can be shown using (A12), (A18) and (A21) that

$$\sigma_A = E_A \epsilon_A + 2\nu_A \sigma_T - E_A \alpha_A \Delta T, \quad (\text{A23})$$

where E_A , ν_A and α_A are the effective axial modulus, Poisson's ratio and axial thermal expansion coefficient respectively, for the concentric cylinder system representing the unidirectional composite, defined by

$$E_A = E_A^* + 2\lambda (\nu_A^m - \nu_A^f)^2 V_f V_m, \quad (\text{A24})$$

$$\nu_A = \nu_A^* - \frac{\lambda}{2} \left(\frac{1}{k_T^m} - \frac{1}{k_T^f} \right) (\nu_A^m - \nu_A^f) V_f V_m, \quad (\text{A25})$$

$$E_A \alpha_A = E_A^* \alpha_A^* + 2\lambda (\nu_A^m - \nu_A^f) (\alpha_T^m + \nu_A^m \alpha_A^m - \alpha_T^f - \nu_A^f \alpha_A^f) V_f V_m, \quad (\text{A26})$$

where

$$E_A^* = V_f E_A^f + V_m E_A^m, \quad (\text{A27})$$

$$E_A^* \alpha_A^* = V_f E_A^f \alpha_A^f + V_m E_A^m \alpha_A^m, \quad (\text{A28})$$

$$\nu_A^* = V_f \nu_A^f + V_m \nu_A^m. \quad (\text{A29})$$

Appendix B: Separation condition for a sliding interface

Consider the concentric cylinder model of a composite where the fibre is broken or matrix is cracked. Following fracture, interface sliding is assumed to have occurred such that extensive sliding has resulted either when fracture first occurred, or following subsequent loading of the composite. For such large scale sliding conditions, it is of interest to determine the critical loading conditions that correspond to the separation of the fibre and matrix at the interface in the regions close to the fibre fracture or matrix crack when stress transfer is governed by the Coulomb friction law. Interface separation takes place when $\sigma_{rr}^f = \sigma_{rr}^m = 0$ on $r = R$.

The displacement field is assumed to have the following form

$$u_r^f = A'_f r, u_\theta^f \equiv 0, u_z^f = \varepsilon_A^f z, \quad (\text{B1})$$

$$u_r^m = A'_m r + \frac{\phi'}{2\mu_T^m r}, u_\theta^m \equiv 0, u_z^m = \varepsilon_A^m z, \quad (\text{B2})$$

where A'_f , A'_m and ϕ' are constants to be determined and ε_A^f and ε_A^m are the uniform axial strain in the fibre and matrix respectively. On differentiating the displacement field it follows that the non-zero strain components are

$$\varepsilon_{rr}^f = \frac{\partial u_r^f}{\partial r} = A'_f, \varepsilon_{\theta\theta}^f = \frac{u_r^f}{r} = A'_f, \varepsilon_{zz}^f = \varepsilon_A^f, \quad (\text{B3})$$

$$\varepsilon_{rr}^m = \frac{\partial u_r^m}{\partial r} = A'_m - \frac{\phi'}{2\mu_T^m r^2}, \varepsilon_{\theta\theta}^m = \frac{u_r^m}{r} = A'_m + \frac{\phi'}{2\mu_T^m r^2}, \varepsilon_{zz}^m = \varepsilon_A^m. \quad (\text{B4})$$

Since from the stress-strain relations

$$\varepsilon_{\theta\theta}^f - \varepsilon_{rr}^f = \frac{1}{2\mu_T^f} (\sigma_{\theta\theta}^f - \sigma_{rr}^f), \quad \varepsilon_{\theta\theta}^m - \varepsilon_{rr}^m = \frac{1}{2\mu_T^m} (\sigma_{\theta\theta}^m - \sigma_{rr}^m), \quad (\text{B5})$$

it can be shown that

$$\sigma_{rr}^f = \sigma_{\theta\theta}^f = \sigma_T - V_m \frac{\phi'}{R^2}, \quad (\text{B6})$$

$$\sigma_{rr}^m = \sigma_T + \phi' \left(\frac{1}{a^2} - \frac{1}{r^2} \right), \quad \sigma_{\theta\theta}^m = \sigma_T + \phi' \left(\frac{1}{a^2} + \frac{1}{r^2} \right). \quad (\text{B7})$$

In the axial direction it is assumed that

$$\sigma_A^f = \frac{(1 + \xi)\sigma_A}{2V_f}, \quad \sigma_A^m = \frac{(1 - \xi)\sigma_A}{2V_m}. \quad (\text{B8})$$

When $\xi = 1$ a matrix crack is being considered as $\sigma_A^m = 0$, and when $\xi = -1$ a fibre fracture is being considered as $\sigma_A^f = 0$. The axial stress-strain relations then lead to

$$\sigma_A^f = \frac{(1 + \xi)\sigma_A}{2V_f} = E_A^f(\epsilon_A^f - \alpha_A^f \Delta T) + 2\nu_A^f \left(\sigma_T - V_m \frac{\phi'}{R^2} \right), \quad (\text{B9})$$

$$\sigma_A^m = \frac{(1 - \xi)\sigma_A}{2V_m} = D_A^m(\epsilon_A^m - \alpha_A^m \Delta T) + 2\nu_A^m \left(\sigma_T + V_f \frac{\phi'}{R^2} \right). \quad (\text{B10})$$

The substitution of (B3), (B4) and (B6)-(B10) in the radial stress-strain equations leads to

$$A'_f = \frac{1 - \nu_T^f}{E_T^f} \left(\sigma_T - V_m \frac{\phi'}{R^2} \right) - \frac{\nu_A^f (1 + \xi)\sigma_A}{E_A^f 2V_f} + \alpha_T^f \Delta T, \quad (\text{B11})$$

$$A'_m = \frac{1 - \nu_T^m}{E_T^m} \left(\sigma_T + V_f \frac{\phi'}{R^2} \right) - \frac{\nu_A^m (1 - \xi)\sigma_A}{E_A^m 2V_m} + \alpha_T^m \Delta T, \quad (\text{B12})$$

It now only remains to determine the constant ϕ' which can be specified on applying the continuity condition for the radial displacement. It follows from (B1) and (B2) that

$$A'_f = A'_m + \frac{\phi'}{2\mu_T^m R^2}. \quad (\text{B13})$$

On using (B11) and (B12)

$$\frac{\phi'}{R^2} = \lambda' \left[\left(\frac{1 - \nu_T^f}{E_T^f} - \frac{1 - \nu_T^m}{E_T^m} \right) \sigma_T + \frac{\nu_A^m (1 - \xi)\sigma_A}{E_A^m 2V_m} - \frac{\nu_A^f (1 + \xi)\sigma_A}{E_A^f 2V_f} + (\alpha_T^f - \alpha_T^m) \Delta T \right], \quad (\text{B14})$$

where

$$\frac{1}{\lambda'} = \frac{1 - \nu_T^m}{E_T^m} V_f + \frac{1 - \nu_T^f}{E_T^f} V_m + \frac{1}{2\mu_T^m}. \quad (\text{B15})$$

It should be noted from (B6) that the interfacial radial stress is zero when

$$\frac{\phi'}{R^2} = \frac{\sigma_T}{V_m}. \quad (\text{B16})$$

Since $E_T^m = 2\mu_T^m(1 + \nu_T^m)$, it then follows from (B14) that this occurs when

$$\left(\frac{\nu_A^f}{E_A^f} \frac{1 + \xi}{2V_f} - \frac{\nu_A^m}{E_A^m} \frac{1 - \xi}{2V_m} \right) \sigma_A = -\frac{2}{V_m E_T^m} \sigma_T + (\alpha_T^f - \alpha_T^m) \Delta T. \quad (\text{B17})$$

